

1 Identification of a Mammalian Silicon Transporter

2 Sarah Ratcliffe,^{1*} Ravin Jugdaohsingh,^{1,2*} Julien Vivancos,³ Alan Marron,⁴ Rupesh
3 Deshmukh,⁴ Jian Feng Ma,⁵ Namiki Mitani-Ueno,⁵ Jack Robertson,¹ John Wills,⁶ Mark V
4 Boekschoten,⁷ Michael Müller,⁷ Robert C Mawhinney,⁸ Stephen D Kinrade,⁸ Paul Isenring,⁹
5 Richard R Bélanger,³ and Jonathan J Powell^{1,2}

6
7 ¹Medical Research Council Elsie Widdowson Laboratory, 120 Fulbourn Road, Cambridge,
8 CB1 9NL, United Kingdom.

9 ²Department of Veterinary Medicine, University of Cambridge, Madingley Road, Cambridge,
10 CB3 0ES, United Kingdom.

11 ³Département de Phytologie-Faculté des Sciences de l'Agriculture et de l'Alimentation,
12 Centre de Recherche en Horticulture, Université Laval, Pavillon Paul-Comtois, Québec City,
13 QC G1V 0A6, Canada.

14 ⁴Department of Zoology, University of Cambridge, Cambridge CB2 3EJ, United Kingdom

15 ⁵Institute of Plant Science and Resources, Okayama University, Chuo 2-20-1, Kurashiki 710-
16 0046, Japan.

17 ⁶Mechanistic Studies Division, Environmental Health Sciences & Research Bureau, Health
18 Canada, Ottawa, Ontario, K1A 0K9, Canada.

19 ⁷Nutrition, Metabolism and Genomics Group, Division of Human Nutrition, Wageningen
20 University, The Netherlands.

21 ⁸Department of Chemistry, Lakehead University, Thunder Bay, ON P7B 5E1, Canada.

22 ⁹Nephrology Group L'Hôtel-Dieu de Québec Institution, Department of Medicine, Faculty of
23 Medicine, Université Laval, Québec City, QC G1R 2J6.

24
25 *These two authors contributed equally to this work.

26 Corresponding author: Jonathan Powell, Medical Research Council Elsie Widdowson
27 Laboratory, 120 Fulbourn Road, Cambridge, CB1 9NL, United Kingdom. Email:
28 jonathan.powell@mrc-ewl.cam.ac.uk and jjp37@cam.ac.uk

29 **Abstract:**

30 Silicon (Si) has long been known to play a major physiological and structural role in certain
31 organisms, including diatoms, sponges, and many higher plants, leading to the recent
32 identification of multiple proteins responsible for Si transport in a range of algal and plant
33 species. In mammals, despite several convincing studies suggesting that silicon is an
34 important factor in bone development and connective tissue health, there is a critical lack of
35 understanding about the biochemical pathways that enable Si homeostasis. Here we report the
36 identification of a mammalian efflux Si transporter, namely Slc34a2 (also termed NaPiIIb) a
37 known sodium-phosphate co-transporter, which was upregulated in rat kidney following
38 chronic dietary Si deprivation. Normal rat renal epithelium demonstrated punctate expression
39 of Slc34a2 and when the protein was heterologously expressed in *Xenopus laevis* oocytes, Si
40 efflux activity (i.e. movement of Si out of cells) was induced and was quantitatively similar
41 to that induced by the known plant Si transporter *OsLsi2* in the same expression system.
42 Interestingly, Si efflux appeared saturable over time, but it did not vary as a function of
43 extracellular HPO_4^{2-} or Na^+ concentration, suggesting that Slc34a2 harbors a functionally
44 independent transport site for Si operating in the reverse direction to the site for phosphate.
45 Indeed, in rats with dietary Si depletion-induced upregulation of transporter expression, there
46 was increased urinary phosphate excretion. This is the first evidence of an active Si transport
47 protein in mammals and points towards an important role for Si in vertebrates and explains
48 interactions between dietary phosphate and silicon.

49

50 **Key words:**

51 Silicon, transport, Slc34a2, *Xenopus laevis* oocytes, rat kidneys

52 **Introduction:**

53 Silicon (Si) is the second most abundant element in the Earth's crust, and is ubiquitous in the
54 diet, but the role it plays in mammalian physiology remains unclear. There is substantial
55 evidence for its importance in the normal health and development of bone and connective
56 tissues of vertebrates (6, 25, 43, 45) but a specific physiological and/or metabolic function
57 has not been identified. In particular, proteins responsible for Si transport in mammals remain
58 elusive. Silicon is essential for many algae (*e.g.* diatoms) to produce their exoskeleton and to
59 complete their cell cycle (5, 21). It is also important in many species of plants, with both
60 structural and physiological roles identified (12, 13, 27).

61 The first Si-transporter to be identified (*CjSIT1*) was in the diatom species *Cylindrotheca*
62 *fusiformis* (22), and SITs are now known from a wide range of diatoms (51),
63 choanoflagellates (32) and haptophytes (11). In plants, Si transport occurs through a
64 collaboration of two individual transporter types, one of which is responsible for influx
65 (movement of Si into cell) and the other for efflux (movement of Si out of cell). Influx occurs
66 through an aquaporin (AQP) channel (*e.g.* *Lsi1*, *Lsi6*) whereas efflux occurs through an
67 energy-dependent active transport process driven by a proton gradient (*e.g.* *Lsi2*) (29, 30).
68 Despite the characterization of multiple Si transporters in algae and plants as described, no
69 Si-transporting homologs have been reported in mammals yet (29, 30, 32).

70 Previously, we reported that Sprague Dawley rats on a Si depleted diet massively reduced
71 their urinary Si output to maintain serum and tissue Si levels (24). This was at the expense of
72 phosphorus, which was decreased in serum and bone (24). These findings suggested that the
73 kidney may be actively involved in Si conservation under chronic Si-deprivation and that,
74 somehow, phosphate is lost in the process. Here we report on the mammalian phosphate
75 transport protein, *Slc34a2*, which was upregulated in the kidney of the rats deprived of
76 dietary Si. This protein was found to induce Si efflux activity when expressed in *Xenopus*

77 oocytes and to exhibit structural similarity with Lsi2 in many plants. Identification that
78 Slc34a2 can transport Si provides new evidence for a biological role for this element in
79 mammals and establishes another distinct gene family of Si transporters.

80

81 **Materials and Methods:**

82 *Silicon depletion study.* Kidneys were obtained from the study of Jugdaohsingh *et al.* (24)
83 following 6 months of dietary Si intervention. Three-week old female Sprague-Dawley rats
84 were maintained for 26 weeks on a formulated low-Si feed (~ 3 µg Si/g feed), with either low
85 Si drinking water (~ 15 ng Si/g water; Si deplete group, n=20) or with orthosilicic acid
86 (H₄SiO₄) supplemented in the drinking water (53 µg Si/g water; Si replete group, n=10). A
87 reference group of rats received a normal laboratory maintenance chow diet (B&K Rat and
88 Mouse Standard Diet; B&K Universal Ltd) which is naturally high in Si (322 µg Si/g feed)
89 and tap water (5 µg Si/g water); see reference (24) for diet compositions. This third group of
90 rats is referred to as Si-high reference group. Total Si intakes were 0.17 mg Si/kg body
91 weight/day in the Si deplete group, 4.1 mg Si/kg/day in the Si replete group and 18.5 mg
92 Si/kg/day in the Si-high reference group. After 26 weeks, rats were sacrificed by asphyxiation
93 with carbon dioxide gas as previously described (24). Rats were killed and processed one at a
94 time, with one rat from each group on the same day. Tissues were then harvested, as
95 previously described (24) and stored at -20 °C immediately following harvesting and then at -
96 80 °C for long term storage. All groups of rats and their tissues were treated in precisely the
97 same fashion. Spot urine samples were collected from fasted rats (24). Urinary Si and P
98 analysis was by inductively coupled plasma optical emission spectrometry (ICP-OES), as
99 described below and data were corrected for urinary creatinine (24). As previously described
100 (24) all animal procedures were carried out in accordance with the UK Home Office Animal

101 Scientific Procedures Act 1986 (Scientific Procedures on Living Animals). Use of laboratory
102 animals was approved by King's College London (UK) Animal Ethics Committee and the
103 UK Home Office. For this study, the left kidney from n=10 Si deplete, n=8 Si replete and n=5
104 Si-high reference rats were ground in liquid nitrogen and total RNA was extracted with the
105 Qiagen RNeasy Maxi kit for microarray and quantitative PCR analysis. This part of the study
106 was carried out in 2008.

107 **Gene array analysis.** Five μg total RNA per sample were hybridized to Affymetrix
108 GeneChip Rat Genome 230 2.0 arrays (n=4 Si deplete and n=4 Si replete kidneys). Gene chip
109 robust multi-array analysis (gcRMA) was used to normalize the data including a
110 summarization step based on m-estimator values for the probe sets (58). Modified T-statistics
111 were used to calculate significance of differential gene expression (10, 44) between the Si
112 replete versus Si deplete groups. Genes were selected as 'differentially expressed' when false
113 discovery rate $q < 0.1$ (49). [The microarray dataset has been submitted to the NCBI Gene
114 Expression Omnibus: Accession number: GSE58404.]

115 **Expression studies.** Quantitative Real-Time PCR was used to investigate the expression of
116 relevant transcripts, including that of an internal control (18S), in the full cohort of rat kidney
117 RNAs (n=10 Si deplete, n=8 Si replete, and n=5 Si-high reference group). Transcripts were
118 amplified with the TaqMan Universal protocol for real-time RT-PCR. The primers were
119 TaqMan Gene Expression Assays consisting of a FAM reporter and TaqMan MGB probes.
120 Differences in gene expression between groups were statistically analyzed by unpaired t-test.

121 **Immunohistochemistry.** Kidneys from a normal laboratory maintenance chow fed rat were
122 excised immediately after necropsy and then fixed in 4% PBS buffered paraformaldehyde.
123 The samples were then cryo-protected via sucrose gradient and snap-frozen in iso-pentane
124 cooled on dry ice. The frozen samples were then embedded in Optimal Cutting Temperature

125 compound (VWR, UK). Tissue sections were subsequently cryo-sectioned at 12 μ m
126 thickness, collected on SuperFrost® slides (Thermo Scientific, USA) and allowed to air dry
127 overnight at room temperature. Sections were blocked with normal serum in PBS. Samples
128 were then incubated with primary antibody against Slc34a2 (Genetex) or an appropriately
129 matched isotype control. Primary antibody was then detected by incubation with goat anti-
130 rabbit IgG (H+L) Alexa Fluor® 488 conjugate (Invitrogen, UK) prior to counter-staining the
131 nuclei with Hoechst 33342 (Invitrogen, UK) and the cytoskeleton (f-actin) with phalloidin
132 CF633 (Biotium, USA). Imaging was carried out on Leica SP2 confocal microscope using a
133 1.2NA 63x water immersion lens. Images were collected using Leica Application Suite
134 software. Alongside Slc34a2-antibody stained sections, images of the isotype controls were
135 also collected under identical settings and in ‘matched’ parallel tissue sections. A threshold
136 removing any minor non-specific signal in the isotype controls was then defined, with this
137 threshold subsequently applied identically across all collected images to robustly identify
138 Slc34a2. Staining for Slc34a2 was distinctly punctate so, as well as presentation in as-
139 collected intensity format, images are also presented in binary format (i.e. all Slc34a2 signal
140 that is brighter than isotype threshold shown at maximum intensity). This ‘view’ was
141 included to facilitate visualisation of Slc34a2 locality within the limits of printed image size.

142 ***Urinary P and Si analyses.*** Fasting spot urine samples collected from 6-h fasted rats (n=8 Si
143 deplete, n=5 Si replete and n=6 Si-high reference rats) were digested (in 1:1 mixture of 69%
144 nitric acid and 40% hydrogen peroxide), diluted (1:100) and analysed for total phosphorus by
145 inductively coupled plasma optical emission spectrometry (ICP-OES; Jobin Yvon 2000-2) at
146 214.914 nm with sample-based standards. Urinary Si was analysed by ICP-OES as
147 previously described (24).

148 ***Inter-organism homology of Si-transporters.*** Homology search was performed with
149 BLASTp (3) against plant and diatom sequences in the EMBL/Genbank non-redundant

150 protein database using the default settings (www.ncbi.nlm.nih.gov). BLASTp and tBLASTn
151 were also used to identify homologs in a range of fully sequenced vertebrate genomes from
152 the EMBL/Genbank and Ensembl databases, and also to identify homologs in selected
153 phylogenetically relevant groups where complete genomes were not available (see
154 Supplemental Table 1). An alignment of homologs was generated using MUSCLE
155 (<http://www.ebi.ac.uk/Tools/msa/muscle/>) under the default settings, producing a final
156 alignment of 38 sequences from 17 species. ProtTest (1) found that the JTT+G+I model
157 provided the best fit to the data under the Akaike Information Criterion. Maximum likelihood
158 analysis was carried out using PhyML (19). Starting trees were generated by BioNJ, with tree
159 searching using the NNI heuristic methods, and topology and branch lengths optimized in
160 ML calculations. One hundred bootstrap datasets were analyzed using the same model and
161 method as for the PhyML analysis, with bootstrap proportions added as numbers to the nodes
162 of the PhyML tree. The alignment was also used for Bayesian MCMC analysis using
163 Phylobayes 3.3 (26), under the CAT +G+I model until convergence (maximum discrepancy
164 <0.3, effective size >100), for 15 parallel chains with sampling every 100 cycles and a burn-
165 in equal to one-fifth the total size of the chain. Posterior probabilities were used to express
166 the support for the nodes in the Bayesian phylogeny. The trees generated were viewed using
167 FigTree v1.3.1 (Andrew Rambaut, Institute of Evolutional Biology, University of Edinburgh
168 2006-2009).

169 ***Calculated Oxoacid volumes.*** The structure for each oxoacid/oxoanion was optimized using
170 the PBE0 functional (2, 38, 39) and 6-31++g(d,p) atomic orbital basis set (4, 9, 15, 16, 20, 41,
171 42). The electron density corresponding to these optimized structures was used to estimate
172 the molecular volume that describes the solvent accessible surface, defined as the volume
173 bounded by a density contour of 0.001 electrons/Bohr³. An increased density of points was
174 used to ensure a more accurate integration so that the computed molecular volumes are

175 quantitative (37, 56). Since these species are in an aqueous environment, structures were
176 optimized within a solvent field using the integral equation formalism variant of the
177 polarizable continuum model (7, 52, 57) to account implicitly for the effects of an aqueous
178 environment on the solvent accessible surface. The Gaussian09 suite of programs (17) was
179 used in these determinations.

180 *Transport activity in Xenopus laevis oocytes*

181 *Cloning the gene of interest and oocyte preparation.* A cDNA sequence verified *Rattus*
182 *norvegicus* IMAGE clone pExpress-1/Slc34a2 (Unigene ID: Rn.16933, Entrez Gene: 84395
183 in DH10BTonA) was purchased from Source BioScience LifeSciences (Cambridge, UK).

184 For synthesis of capped RNA, the open reading frame (ORF) was amplified by PCR with the
185 following primers: 5'- GAGGATCCATGGCTCCTTGGCCCGAGTTG-3' and 5'-
186 GAGGATCCTAGAACACTGTAGTGTGGACA-3'. The fragment containing the ORF
187 was inserted into the *Bgl*III site of a *Xenopus* oocytes expression vector pXβG-ev1 (a pSTP64
188 T-derived pBluescript type vector into which *Xenopus* β-globin 5' and 3' UTR had been
189 inserted) (40). Capped RNA was then synthesized from linearized pXβG-ev1 plasmids by *in*
190 *vitro* transcription with mMESSAGE mMACHINE High Yield Capped RNA Transcription
191 Kit (Ambion) according to the manufacturer's instructions.

192 Oocytes were isolated from *Xenopus laevis* frogs purchased from NASCO (Nasco-Fort
193 Atkinson, WI, USA) and from Watanabe Zosyoku (Hyogo Pref, Japan). Procedures for
194 defolliculation, culture condition and selection were the same as described previously (35). A
195 volume of 50 nl of the *in vitro* cRNA transcripts (1 ng/nl) was injected into stage V oocytes
196 using a Nanoject II automatic injector (Drummond Scientific Co.). Water-injected oocytes
197 were used as a negative control, *OsLsi1*-injected oocytes as positive controls while testing for
198 influx activity and *OsLsi2*-injected oocytes while testing for efflux activity. Ethical approval

199 was obtained (permit number 21031043) from the Animal Care Committee of Laval
200 University (Canada).

201 ***Influx transport activity.*** After incubation in a Modified Barth's Saline (MBS) solution (88
202 mM NaCl, 1 mM KCl, 2.4 mM NaHCO₃, 15 mM Tris-HCl at pH 7.6, 0.3 mM Ca(NO₃)₂,
203 0.41 mM CaCl₂, 0.82 mM MgSO₄, 10 µg/ml sodium penicillin, and 10 µg/ml streptomycin
204 sulfate) at 18 °C overnight, the cRNA-injected oocytes were exposed to the MBS solution
205 supplemented with 1 mM H₄GeO₄, 0.1 mM HAsO₄²⁻ or 1 mM HPO₄²⁻ at pH 7.6. Following
206 30 min incubation at 18 °C, the oocytes were washed five times with MBS alone and digested
207 with concentrated (61%) HNO₃. The Ge, As and P concentrations in the digested solutions
208 were determined by ICP-MS (7700X; Agilent Technologies) with appropriate standards, QCs
209 and sample blanks.

210 To investigate the Si influx and its dependence on extracellular [Na⁺] or [HPO₄²⁻], oocytes
211 were incubated for three days at 18 °C in MBS5 (84 mM Na⁺ and 2 mM HPO₄²⁻)
212 supplemented with 100 µM each of penicillin and streptomycin. Then a set of 10 oocytes for
213 each condition was exposed to MBS2 (1.7 mM H₄SiO₄, 10 mM Na⁺ and 0.5 mM HPO₄²⁻) or
214 MBS3 (1.7 mM H₄SiO₄, 84 mM Na⁺ and 2 mM HPO₄²⁻) solution for 2 h. After exposure,
215 oocytes were rinsed in a solution containing 0.32 M sucrose and 5 mM HEPES (pH 7.4) and
216 then digested in 25 µl concentrated nitric acid, dried at 82 °C for 2 h, reconstituted in plasma
217 grade water (100 µl) and 10 µl analyzed by atomic absorption spectroscopy (see below).

218 ***Efflux transport activity.*** To investigate the efflux transport activity for H₄GeO₄ by
219 *RnSlc34a2*, 50 nl 1 mM H₄GeO₄ in MBS was directly injected into *RnSlc34a2* transfected
220 oocytes. The oocytes were then washed five times with MBS and transferred to 200 µl of
221 fresh MBS at 18 °C. H₄GeO₄ was allowed to efflux into the incubation medium. After 30 min
222 and 2 h, the incubation medium was carefully sampled, and at the end of the experiment, the

223 oocytes were digested with concentrated HNO₃ and the samples were analyzed for Ge by
224 ICP-MS (7700X; Agilent Technologies) with appropriate standards, QCs and sample blanks.

225 To investigate the efflux transport activity for Si by *RnSlc34a2*, oocytes were injected with
226 25 nl of 500 ng/nl cRNA of *RnSlc34a2* or *OsLsi2* or an equal volume of H₂O as a negative
227 control. Pools of 10 oocytes were then loaded with Si by incubation for three days at 4 °C in
228 MBS1 or MBS2, both containing 2 mM Si but different concentrations of Na⁺ and HPO₄²⁻
229 (Supplemental Table 2). These were then exposed to fresh MBS without added Si but with
230 different concentrations of Na⁺ and HPO₄²⁻ (MBS, MBS3, MBS4 or MBS5 solution;
231 Supplemental Table 2) for zero, one or two hours. After exposure, oocytes were rinsed in a
232 solution containing 0.32 M sucrose and 5 mM HEPES (pH 7.4), digested with concentrated
233 HNO₃ (25 µl for each pool of 10 oocytes) and dried at 82 °C for 2 h. Plasma-grade water
234 (100 µl) was then added, and samples were incubated for 1 h at room temperature. Samples
235 were vortexed and then centrifuged for 5 min at 13,000 g. 10 µl of samples were then
236 analysed by Zeeman atomic absorption spectrometer (Varian AA240Z;
237 <http://www.varian.com>) equipped with a GTA120 Zeeman graphite tube atomizer, to
238 determine the intracellular Si concentration. Silicon levels in the samples and sample blanks
239 were quantified using appropriate standards prepared using 1,000 ppm ammonium
240 hexafluorosilicate solution (Fisher Scientific, <http://www.fishersci.com>). Data were analyzed
241 with SpectrA software (Varian).

242 ***Statistical analysis.*** Results are reported as means ± SD unless otherwise stated. Linear
243 relationships between dietary Si exposure and the relative renal expression of Slc34 genes
244 were assessed at a significance of $p \leq 0.05$. Thereafter, individual differences were assessed
245 by Independent (unpaired) Samples 2-Tailed T-test. Where there were multiple group
246 comparisons a Bonferroni correction was applied to the p value (i.e. p/n), and significance

247 was taken as $p \leq 0.05/n$. All statistical analysis was conducted in GraphPad Prism (Version
248 6.0b) or IBM SPSS version 21 (IBM Corporation).

249

250 **Results and Discussion:**

251 **Identifying *RnSlc34a2* as a candidate for Si transport.** Data from our study of Si
252 deficiency in rats strongly suggested active urinary conservation of Si during dietary Si
253 depletion (24). The present investigation utilized kidneys harvested during this study to
254 investigate Si regulatory genes. Gene arrays (Affymetrix GeneChip Rat Genome 230 2.0
255 arrays containing over 16,000 Entrez IDs and 11 probes per gene) were performed on RNA
256 extracted from the kidney tissues of Si deplete and Si replete rats (n=4 for each group) and
257 the data were interrogated for differential regulation of potential transporters (Fig. 1a). The
258 gene array findings^{Footnote1} were confirmed by Real-Time RT-PCR analysis and this technique
259 was also subsequently used to investigate a larger cohort of samples from the Si deplete
260 (n=10), Si replete (n=8) and a reference group (n=5) which were rats kept on a normal
261 laboratory chow diet that is naturally high in Si (referred to as Si-high reference group).
262 *Slc34a2* (type II sodium-phosphate co-transporter), commonly referred to as NaPi-IIb, was
263 expressed especially highly in the kidneys of rats on the Si deplete diet (2.8 and 4.8 fold
264 higher than for kidneys from rats on the Si replete and Si-high reference diets, respectively;
265 Fig. 1b). mRNA expression of other *Slc34* family members, namely *Slc34a1* and *Slc34a3*,
266 were unchanged with dietary Si intervention (inset, Fig. 1b).

267 Correlation between *Slc34a2* expression and urinary Si concentration, showed an inverse
268 exponential relationship between fasting urinary Si level and the relative expression of
269 *Slc34a2* (Fig. 2), implying that *Slc34a2* is involved in the reabsorption of H_4SiO_4 from the

270 pre-urine under dietary Si deprivation. No such relationship was observed for Slc34a1 and
271 Slc34a3, or other candidate transporters identified in the gene arrays (Fig. 1a).

272 Only a few reports have demonstrated the renal expression of Slc34a2. The original paper
273 characterising the transporter demonstrated its presence in murine kidney at the mRNA level
274 (23). Suyama *et al.* confirmed this more recently by *in situ* hybridization as well as protein
275 expression and localisation by antibody staining (50). The kidney samples from our study
276 were not adequately collected for immunohistochemical analysis, but were for RNA analysis.
277 Thus we confirmed with appropriately collected kidneys from a control rat that, as previously
278 published (50), Slc34a2 protein is expressed by the tubular epithelial cells of the kidney
279 cortex (Fig. 3). Here, as previously reported (50), Slc34a2 showed distinct punctate staining:
280 some of which was basolateral within the cell and some of which was apical/cytosolic (Fig.
281 3). Whether silicate deficiency dictates only the level of expression of Slc34a2 (Fig. 1) or,
282 also its precise location in the cell, as excess dietary phosphate does (50), should be
283 investigated in future work.

284 Finally, to translate these observations (i.e. that Slc34a2 has some basolateral expression in
285 kidney cells and is upregulated in Si deplete diets) we measured urinary P excretion in the
286 three groups. The Si-high reference group diet was higher in P than the Si replete group diet,
287 being 7.0 versus 2.3 mg/g respectively, and so, as expected, urinary P excretion was
288 significantly reduced in the latter (by 89 mg/mmol creatinine for the medians; $p = 0.008$; $n = 6$
289 and 5 respectively (Fig 4)). However, the Si deplete group (with the same dietary P level as
290 the Si replete group) showed no difference in urinary P levels compared to the reference
291 group (Fig. 4), showing that in this group, phosphate was being (relatively) wasted as a
292 consequence of Si being conserved.

293 ***RnSlc34a2* transport activity.** The ubiquitous nature of Si makes transport studies of soluble
294 silicic acid (H_4SiO_4) challenging. It is well known that related oxoacids may ride the same

295 transport systems (22, 29, 36, 54) owing to similarities in their structure and solvated
296 molecular volume (Table 1). Germanic acid (H_4GeO_4), the closest structural analogue of
297 silicic acid, is therefore often employed as a proxy for Si transport, thereby avoiding all
298 background and contamination issues with Si and facilitating analysis (22, 29). Recently,
299 however, graphite furnace atomic absorption spectrometry (GFAAS) was shown to be
300 effective for directly measuring Si influx/efflux in *Xenopus laevis* oocytes transfected with
301 Si-transporting aquaporins from plants (8, 18). Hence, both methods of characterizing Si
302 transport – indirect and direct – were used in the present investigation.

303 The Slc34a2 coding sequence was inserted into a *Xenopus laevis* expression vector, and
304 cRNA synthesized from this construct was injected into oocytes. Initial expression and
305 plasma membrane localization were verified using an eGFP tagged Slc34a2 construct.
306 Slc34a2 is recognised as a sodium phosphate importer, especially in the brush border of small
307 intestine membrane cells (14, 31, 36, 55), and arsenate also rides this transport system (36,
308 54). Therefore, both of these oxoacids were utilized as easily-measured probes to confirm
309 Slc34a2 influx activity (Fig. 5a & 5b). The rice Si importer, *OsLsi1*, was used as a positive
310 control and was found to promote both H_4SiO_4 (Fig. 5c) and H_4GeO_4 (Fig. 6a) influx. By
311 contrast, no influx of either H_4SiO_4 or H_4GeO_4 by Slc34a2-expressing oocytes was observed
312 (Fig. 5c & Fig. 6a). On the other hand, efflux of both H_4SiO_4 and H_4GeO_4 was detected for
313 oocytes expressing Slc34a2 (Fig. 5e & Fig. 6b, respectively) as well as those expressing rice
314 Si exporter *OsLsi2*, which was employed as a positive efflux control. Of note, the magnitude
315 of fractional H_4SiO_4 efflux after two hours was quantitatively similar between Slc34a2 and
316 *OsLsi2*.

317 Given that inward phosphate (HPO_4^{2-}) transport by Slc34a2 is coupled to the inward
318 transport of three sodium ions (i.e. it is electrogenic (14, 55)), we investigated how varying
319 the concentrations of Na^+ and HPO_4^{2-} in the external medium might influence Si influx and

320 efflux in Slc34a2-expressing oocytes. No significant effects were observed at the broad
321 concentrations investigated (Fig. 5d & Fig. 5f). These findings suggest that Si is not
322 translocated across the membrane through the Na^+ or HPO_4^{2-} transport site, but through an
323 independent transport site that is potentially involved in Si efflux primarily. In keeping with
324 this possibility is the presence of multiple, often independent binding sites in a number of
325 ABCD family members (47). Alternatively, Slc34a2 could cooperate with accessory proteins
326 to promote Si efflux. In this regard, the Na^+/K^+ -ATPase gamma subunit FXYD2 appears to
327 play a role in Mg^{2+} transport, while the alpha and beta subunits alone do not exhibit such
328 transport capabilities (46).

329 **Homology between Slc34a2 and Si transporters.** Comparative sequence analysis of
330 Slc34a2 indicated no significant homology with known plant or algal Si transporters.
331 However, marked similarities were revealed upon pairwise alignment of the transmembrane
332 domains of Slc34a2 and the plant Si efflux transporter Lsi2 (Fig. 7), thereby suggesting a
333 conserved structure among Si efflux proteins.

334 **Phylogenetic analysis of the Slc34 family.** Sequence alignment within the rat Slc34 gene
335 family led to the identification of a ~30-residue stretch that is only present in Slc34a2. Given
336 that Slc34a1 and Slc34a3 were not upregulated under Si deprivation, this finding points
337 towards the possibility that the ~30-residue stretch conveys Si-transport activity to Slc34a2
338 (Fig. 1c and Table 2).

339 Phylogenetic analysis of the Slc34a genes from a range of vertebrates (Supplementary Table
340 1 & Fig. 8) showed that the family underwent an expansion relatively early in vertebrate
341 evolution, resulting in three distinct main groups (a1, a2, and a3) among the modern jawed
342 vertebrates. At least one member of the a2-group was found in all of the jawed vertebrate
343 genomes searched. In contrast, losses of the a1- and a3-group genes were observed in several

344 fully-sequenced genomes (e.g. zebrafish, chicken). This would suggest that the Slc34a2-
345 group genes have a unique or important role whose loss cannot be complemented for by other
346 transporters, and that this function is conserved across the jawed vertebrates. Common to all
347 members of the Slc34a2 group, and to the homologous Slc34a2 gene in the lamprey, is a
348 motif containing three positive amino acid residues (R, H or K) separated by smaller
349 uncharged residues (commonly C or S) (Fig. 9). This motif aligns with the unique predicted
350 transmembrane domain noted above in the rat Slc34a2 gene (Fig. 1c and Table 2), and points
351 towards an important functional role. Conserved positively charged amino acids have been
352 noted in other Si-related proteins, such as the GRQ motifs of the SIT active Si transporters
353 (32, 51). It may be postulated that these residues interact with local negative charges on the
354 silicic acid molecule as part of a general biochemical basis for transmembrane Si transport.

355

356 **Conclusions**

357 The identification that Slc34a2 can transport Si in mammals establishes another distinct gene
358 family of Si-transporters that could be involved in regulation of Si homeostasis and that bears
359 no sequence similarity with known Si-related genes in plants, sponges, choanoflagellates or
360 diatoms, although it shows strong structural similarities to silicon exporters in plants.
361 Crucially, our work is also one of the first pieces of evidence for a functionally relevant Si-
362 responsive gene in mammals. In parallel with this work, Garneau *et al.* (18) and Deshmukh *et*
363 *al* (8) have recently identified Si-permeable aquaporins that appear to play an important role
364 in Si influx. Coupled with the active efflux transporter that is reported herein, we propose a
365 Si transport model in mammals that mirrors that known in plants (28), i.e., a model in which
366 an influx and efflux transporter must be present to allow Si movement through cells. Here,
367 Slc34a2 is effluxing H_4SiO_4 from the renal tubular epithelial cell into the circulation, i.e. it is

368 involved in the reabsorption of H_4SiO_4 in the kidneys. As an inevitable consequence of this
369 expression at this cellular location, phosphate will be moved in the opposing direction.
370 Dietary Si-P interactions have been noted, with animals on a Si deficient diet showing
371 conserved bone Si levels but depleted bone P levels (24). Assuming Slc34a2 is similarly
372 involved in bone-conservation of Si as it is in the kidney then our results explain these
373 observation (24). Finally, it is also interesting to note that Lsi2's are equally upregulated in
374 plants in conditions of Si deprivation (34), a phenomenon that was instrumental in identifying
375 Slc34a2 in this work. Collectively our data provide indication that, rather than being a
376 biochemically-inert element, Si in fact plays a role in vertebrate physiology deserving of its
377 preservation under exposure conditions of deprivation.

378 **Acknowledgements:**

379 We thank Dr Paul Curnow (University of Bristol, UK) and Dr Joanne Marks and Professor
380 Robert Unwin (University College London, UK) for discussions and comments on the
381 manuscript. The *Xenopus laevis* oocyte entry vector pT7TS (used for the Si transport studies)
382 was a kind gift from Dr Tony Miller (Rothamsted Research Institute, UK).

383 **Current addresses:**

384 Sarah Ratcliffe: University of Bristol, School of Biochemistry, Medical Sciences Building,
385 University Walk, Bristol BS8 1TD.

386 Alan Marron: University of Cambridge, Department of Applied Maths and Theoretical
387 Physics, Centre for Mathematical Sciences, Wilberforce Road, Cambridge CB3 0WA.

388 Michael Müller: University of East Anglia, Norwich Medical School, Faculty of Medicine
389 and Health Sciences, Norwich NR4 7TJ.

390 **Grants:**

391 This work was supported by: Medical Research Council (grant number
392 MC_US_A090_0008/Unit Programme number U1059) (J.J.P); Charitable foundation of the
393 Institute of Brewing and Distilling, UK (S.R. & R.J.); Grant-in-Aid for Scientific Research
394 on Innovative Areas from the Ministry of Education, Culture, Sports, Science and
395 Technology of Japan (No. 22119002) (J.F.M & N.M.U); BBSRC Comparative Genomics
396 training grant BB/E527604/1 and a Leathersellers' Company Scholarship awarded by
397 Fitzwilliam College, Cambridge (A.M); Natural Sciences and Engineering Research Council
398 of Canada (No. 364175) and Canada Foundation for Innovation (No. 950-205342) (J.V, R.D,
399 R.R.B); Netherlands Nutrigenomics Centre (M.V.B & M.M); and Natural Sciences and
400 Engineering Research Council of Canada (S.D.K). Canadian Institute of Health and Research
401 (P.I.)

402 **Disclosures:**

403 The authors have no conflicts of interest.

404 **Author Contributions:**

405 J.J.P, R.J, and S.R devised the competitive renal gene expression approach in Si deficiency

406 and sufficiency and strategically led the overall hypothesis with input from S.D.K. M.V.B

407 and M.M performed transcriptomic analysis and interpretation of transcriptomics data.

408 N.M.U and J.F.M designed and performed the Ge, As, and P influx experiments. R.R.B, R.D,

409 and J.V identified that Slc34a2 could have Si export activity and undertook the Si transport

410 experiments in *Xenopus* oocytes with input from P. I. S.R and A.M produced the Slc34a2-

411 GFP-pT7TS plasmid construct, verified *Xenopus* expression by fluorescent microscopy, and

412 performed the phylogenetic and bioinformatics analysis. J.R and J.W performed the IHC

413 analysis and helped with interpretation of the data. R.C.M. undertook the oxoacid and

414 oxoanion calculations. All authors contributed towards writing the manuscript.

415 **Footnote:**

416 Gene array data has been submitted to the GEO repository and assigned the reference

417 GSE58404.

418 **References:**

- 419 1. Abascal F, Zardoya R, Posada D. ProtTest: selection of best-fit models of protein
420 evolution. *Bioinformatics* 21:2104–2105, 2005.
- 421 2. Adamo C, Barone V. Toward reliable density functional methods without adjustable
422 parameters: The PBE0 model. *J Chem Phys* 110:6158-6169, 1999.
- 423 3. Altschul SF, Madden TL, Schäffer AA, Zhang J, Zhang Z, Miller W, Lipman DJ.
424 Gapped BLAST and PSI-BLAST: a new generation of protein database search
425 programs. *Nucleic Acids Res* 25:3389–3402, 1997.
- 426 4. Binning Jr. RC, Curtiss, LA. Compact contracted basis-sets for 3rd-row atoms - GA-
427 KR. *J Comp Chem* 11:1206-16, 1990.
- 428 5. Brzezinski MA, Olson RJ, Chisholm SW. Silicon availability and cell-cycle
429 progression in marine diatoms. *Mar. Ecol Prog Ser* 67:83–96, 1990.
- 430 6. Carlisle EM. Silicon: an essential element for the chick. *Science* 178:619-621, 1972.
- 431 7. Cossi M, Rega N, Scalmani G, Barone V. Energies, structures, and electronic properties
432 of molecules in solution with the C-PCM solvation model. *J Comp Chem* 24:669-681,
433 2003.
- 434 8. Deshmukh RK, Vivancos J, Ramakrishnan G, Guerin V, Carpentier G, Sonah H, Labbe
435 C, Isenring P, Belzile FJ, Bélanger RR. A precise spacing between NPA domains of
436 aquaporins is essential for silicon permeability in plants. *Plant J*
437 DOI:10.1111/tpj.12904, 2015.
- 438 9. Ditchfield R, Hehre WJ, Pople JA. Self-consistent molecular orbital methods. 9.
439 Extended gaussian-type basis for molecular-orbital studies of organic molecules. *J*
440 *Chem Phys* 54:724, 1971.
- 441 10. Duncan AE, Munn-Chernoff MA, Hudson DL, Eschenbacher MA, Agrawal A, Grant
442 JD, Nelson EC, Waldron M, Glowinski AL, Sartor CE, Bucholz KK, Madden PAF,
443 Heath AC. Genetic and Environmental Risk for Major Depression in African-American
444 and European-American Women. *Twin Res Hum Genet* 17:244-253, 2014.
445 doi:10.1017/thg.2014.28.
- 446 11. Durak GM, Taylor AR, Walker CE, Audic S, Schroeder D, Probert I, Vargas C de.,
447 Brownlee C, Wheeler GL. A role for diatom-like silicon transporters in calcifying
448 coccolithophores. *Nat Commun* 7:10543, 2016.
- 449 12. Epstein E. The anomaly of silicon in plant biology. *Proc Natl Acad Sci USA* 50:641-
450 664, 1994.
- 451 13. Fauteux F, Chain F, Belzile F, Menzies JG, & Bélanger RR. The protective role of
452 silicon in the Arabidopsis-powdery mildew pathosystem. *Proc Natl Acad Sci USA*
453 103:17554–17559, 2006.
- 454 14. Forster IC, Hernando N, Biber J, Murer H. Proximal tubular handling of phosphate: a
455 molecular perspective. *Kid Int* 70:1548-1559, 2006.
- 456 15. Franci MM, Pietro WJ, Hehre WJ, Binkley S, Gordon MS, DeFrees DJ, Pople JA. Self-
457 consistent molecular orbital methods. 23. A polarization-type basis set for 2nd-row
458 elements. *J Chem Phys* 77:3654-3665, 1982.

- 459 16. Frisch MJ, Pople JA, Binkley JS. Self-consistent molecular orbital methods. 25.
460 Supplementary functions for gaussian basis sets. *J Chem Phys* 80:3265-3269, 1984.
- 461 17. Frisch MJE, Trucks GW, Schlegel Hs B, Scuseria GE, Robb MA, Cheeseman JR,
462 Scalmani G, Barone V, Mennucci B, ea Petersson GA, Nakatsuji H, Caricato M, Li X,
463 Hratchian HP, Izmaylov AF, Bloino J, Zheng G, Sonnenberg JL, Hada M, Ehara M,
464 Toyota K, Fukuda R, Hasegawa J, Ishida M, Nakajima T, Honda Y, Kitao Oxx, Nakai
465 H, Vreven T, Montgomery Jr JA, Peralta JE, Ogliaro F o, Bearpark M, Heyd JJ,
466 Brothers, KN Kudin, VN Staroverov, R Kobayashi, J Normand, K Raghavachari, A
467 Rendell E, Burant JC, Iyengar SS, Tomasi J, Maurizio Cossi, Rega N, Millam JM,
468 Klene M, Knox JE, Cross JB, Bakken V, Adamo C, Jaramillo J, Gomperts R,
469 Stratmann RE, Yazyev O, Austin AJ, Cammi R, Pomelli C, Ochterski JW, Martin RL,
470 Morokuma K, Zakrzewski VG, Voth GA, Salvador P, Dannenberg JJ, Dapprich S,
471 Daniels AD, Farkas aÖ, Foresman JB, Vincent Ortiz J, Cioslowski J, Fox DJ. Gaussian
472 09, Revision D.01, 2009.
- 473 18. Garneau AP, Carpentier GA, Marcoux AA, Frenette-Cotton R, Simard CF, Remus-
474 Borel W, Caron L, Jacob-Wagner M, Noel M, Powell JJ, Belanger R, Cote F, Isenring
475 P. Aquaporins mediate silicon transport in humans. *PLOS One* 10:e0136149, 2015.
- 476 19. Guindon S, Dufayard JF, Lefort V, Anisimova M, Hordijk W, Gascuel O. New
477 algorithms and methods to estimate maximum-likelihood phylogenies: assessing the
478 performance of PhyML 3.0. *Syst Biol* 59:307–321, 2010.
- 479 20. Hehre WJ, Ditchfield R, Pople JA. Self-consistent molecular orbital methods. 12.
480 Further extensions of gaussian-type basis sets for use in molecular-orbital studies of
481 organic-molecules. *J Chem Phys* 56:2257, 1972.
- 482 21. Hildebrand M, Higgins DR, Busser K, Volcani BE. Silicon-responsive cDNA clones
483 isolated from the marine diatom *Cylindrotheca fusiformis*. *Gene* 132:213–218, 1993.
- 484 22. Hildebrand M, Volcani BE, Gassmann W, Schroeder JI. A gene family of silicon
485 transporters. *Nature* 385:688–689, 1997.
- 486 23. Hilfiker H, Hattenhauer O, Traebert M, Forster I, Murer H, Biber J. Characterization of
487 a murine type II sodium-phosphate cotransporter expressed in mammalian small
488 intestine. *Proc Natl Acad Sci USA* 95:14564-14569, 1998.
- 489 24. Jugdaohsingh R, Calomme MR, Robinson K, Nielsen F, Anderson SHC, D’Hease P,
490 Geutsens P, Loveridge N, Thompson RPH, Powell JJ. Increased longitudinal growth in
491 rats on a silicon-depleted diet. *Bone* 43: 96–606, 2008.
- 492 25. Jugdaohsingh R, Tucker KL, Qiao N, Cupples LA, Kiel DP, Powell JJ. Dietary silicon
493 intake is positively associated with bone mineral density in men and premenopausal
494 women of the Framingham Offspring cohort. *J Bone Miner Res* 19:297–307, 2004.
- 495 26. Lartillot N, Philippe H. A Bayesian mixture model for across-site heterogeneities in the
496 amino-acid replacement process. *Mol Biol Evol* 21:1095–1109, 2004.
- 497 27. Ma JF, Tamai K, Ichii M, Wu GF. A rice mutant defective in Si uptake. *Plant Physiol*
498 130:2111–2117, 2002.
- 499 28. Ma JF, Yamaji, N. A cooperative system of silicon transport in plants. *Trends Plant Sci*
500 20(7):435-442, 2015.
- 501 29. Ma JF, Tamai K, Yamaji N, Mitani N, Konishi S, Katsuhara M, Ishiguro M, Murata Y,
502 Yano M. A silicon transporter in rice. *Nature* 440:688–91, 2006.

- 503 30. Ma JF, Yamaji N, Mitani N, Tamai K, Konishi S, Fujiwara T, Katsuhara M, Yano M.
504 An efflux transporter of silicon in rice. *Nature* 448:209–12, 2007.
- 505 31. Marks J, Debman ES, Unwin RJ. Phosphate homeostasis and the renal-gastrointestinal
506 axis. *Am J Physiol Renal Physiol* 299:F285-F296, 2010.
- 507 32. Marron AO, Alston MJ, Heavens D, Akam M, Caccamo M, Holland PWH, Walker G.
508 A family of diatom-like silicon transporters in the siliceous loricate choanoflagellates.
509 *Proc Biol Sci* 280:20122543, 2013.
- 510 33. Meyer A, Zardoya R. Recent Advances in the (Molecular) Phylogeny of the
511 Vertebrates. *Ann. Rev. Ecol Evol Syst* 34:311–338, 2003.
- 512 34. Mitani N, Chiba Y, Yamaji N, Ma JF. Identification and characterization of maize and
513 barley Lsi2-like silicon efflux transporters reveals a distinct silicon uptake system from
514 that in rice. *The Plant Cell* 21:2133-2142, 2009.
- 515 35. Mitani N, Yamaji N, Ma JF. Characterization of substrate specificity of a rice silicon
516 transporter, Lsi1. *Pflugers Arch - Eur J Physiol* 456:679–86, 2008.
- 517 36. Murer H, Forster I, Biber, J. The sodium phosphate cotransporter family SLC34.
518 *Pflugers Arch. - Eur J Physiol* 447:763–7, 2004.
- 519 37. Onsager L. Electric moments of molecules in liquids. *J Am Chem Soc* 58:1486-1493,
520 1936.
- 521 38. Perdew JP, Burke K, Ernzerhof M. Errata: Generalized gradient approximation made
522 simple. *Phys Rev Lett* 78:1396, 1997.
- 523 39. Perdew JP, Burke K, Ernzerhof M. Generalized gradient approximation made simple.
524 *Phys Rev Lett* 77:3865-3868, 1996.
- 525 40. Preston GM, Carroll TP, Guggino WB, Agre P. Appearance of water channels in
526 *Xenopus* oocytes expressing red cell CHIP28 protein. *Science* 256:385–387, 1992.
- 527 41. Rassolov VA, Pople JA, Ratner MA, Windus, TL. 6-31G* basis set for atoms K
528 through Zn. *J Chem Phys* 109:1223-1229, 1998.
- 529 42. Rassolov VA, Ratner MA, Pople JA, Redfern PC, Curtiss, LA. 6-31G* basis set for
530 third-row atoms. *J Comp Chem* 22:976-84, 2001.
- 531 43. Reffitt DM, Ogston N, Jugdaohsingh R, Cheung HFJ, Evans BAJ, Thompson RPH,
532 Powell JJ, Hampson GN. Orthosilicic acid stimulates collagen type 1 synthesis and
533 osteoblastic differentiation in human osteoblast-like cells in vitro. *Bone* 32:127–135,
534 2003.
- 535 44. Sartor MA, Tomlinson CR, Wesselkamper SC, Sivaganesan S, Leikauf GD,
536 Medvedovic M. Intensity-based hierarchical Bayes method improves testing for
537 differentially expressed genes in microarray experiments. *BMC Bioinformatics* 7:538,
538 2006.
- 539 45. Schwarz K, Milne DB. Growth-promoting Effects of Silicon in Rats. *Nature* 239:333–
540 334, 1972.
- 541 46. Sha Q, Pearson W, Burcea LC, Wigfall DA, Schlesinger PH, Nichols CG, Mercer RW.
542 Human FXVD2 G41R mutation responsible for renal hypomagnesemia behaves as an
543 inward-rectifying cation channel. *Am J Physiol Renal Physiol* 295 (1):F91-9, 2008.
- 544 47. Shilton BH. Active transporters as enzymes: an energetic framework applied to major
545 facilitator superfamily and ABC importer systems. *Biochem J* 467(2):193-9, 2015.

- 546 48. Stamm M, Staritzbichler R, Khafizov K, Forrest LR. Alignment of helical membrane
547 protein sequences using AlignMe. *PLoS ONE* 8:e57731, 2013.
- 548 49. Storey JD, Tibshirani R. Statistical significance for genomewide studies. *Proc Natl*
549 *Acad Sci USA* 100:9440–9445, 2003.
- 550 50. Suyama T, Okada S, Ishijima T, Iida K, Abe K, Nakai Y. High phosphorus diet-
551 induced changes in NaPi-IIb phosphate transporter expression in the rat kidney: DNA
552 microarray analysis. *PLoS ONE* 7:e29483, 2012.
- 553 51. Thamtrakoln K, Alverson AJ, Hildebrand M. Comparative sequence analysis of
554 diatom silicon transporters: toward a mechanistic model of silicon transport. *J Phycol*
555 42:822–834, 2006.
- 556 52. Tomasi J, Mennucci B, Cancès E. The IEF version of the PCM solvation method: An
557 overview of a new method addressed to study molecular solutes at the QM ab initio
558 level. *J Mol Struct (Theochem)* 464:211-226, 1999.
- 559 53. Viklund H, Elofsson A. OCTOPUS: improving topology prediction by two-track ANN-
560 based preference scores and an extended topological grammar. *Bioinformatics*
561 24:1662–8, 2008.
- 562 54. Villa-Bellosta R, Sorribas V. Role of rat sodium/phosphate cotransporters in the cell
563 membrane transport of arsenate. *Toxicol Appl Pharmacol* 232:125–34, 2008.
- 564 55. Wagner CA, Hernando N, Forster IC, Biber J. The SLC34 family of sodium-dependent
565 phosphate transporters. *Pfugers Archiv Eur J Physiol* 466:139-153, 2014.
- 566 56. Wong MW, Frisch MJ, Wiberg KB. Solvent effects 1. The mediation of electrostatic
567 effects by solvents. *J Am Chem Soc* 113:4776-4782, 1991.
- 568 57. Wong MW, Wiberg KB, Frisch MJ. Hartree-Fock second derivatives and electric field
569 properties in a solvent reaction field - theory and application. *J Chem Phys* 95:8991-
570 8998, 1991.
- 571 58. Wu Z, Irizarry RA, Gentleman R, Murillo FM, Spencer F. A model based background
572 adjustment for oligonucleotide expression arrays. *J Amer Stat Assoc* 99:909–917, 2004.

573 **Figure Captions and Tables:**

574 **Figure 1. Identifying *RnSlc34a2* as a candidate for Si transport. (a)** Relative expression
575 of solute-like carriers in the kidney of *Rattus norvegicus* from Si deplete (n=4) compared
576 with Si replete (n=4) animals. Data was analysed by gene array. Red indicates up-regulation
577 and blue down-regulation of expression; Si replete versus Si deplete group. Multiple probe
578 sets per gene can be present as was the case for *Slc13a1*. **(b)** Quantitative PCR analysis of
579 *Slc34a2* and of family members (inset) in the kidneys of Si-high reference, Si replete and Si
580 deplete rats. Overall, the relative expression of *RnSlc34a2* was inversely related to dietary Si
581 exposure ($p < 0.05$), but there was no relationship with *Slc34a1* or *Slc34a3* ($p = 0.5$ and 0.4
582 respectively). Gene expressions are relative to the Si-high reference group. **(c)** Sequence
583 alignment of the *Rattus norvegicus* *Slc34* gene family. *Slc34a2* is characterized by a ~30-
584 residue stretch (highlighted in yellow) that is not present in *Slc34a1* and *Slc34a3*. Asterisks
585 (*) below sequence indicate identical amino acids, colons (:) indicate functionally similar
586 amino acids and dashes (-) indicate gaps in the alignment.

587

588 **Figure 2. Correlation between renal *RnSlc34a2* expression (by quantitative RT PCR**
589 **analysis) and fasting urinary Si excretion.** Urinary Si excretion in the rats (Si deplete
590 (*squares*), Si replete (*circles*) and lab chow reference group (Si-high reference; *triangles*)
591 showed an inverse relationship with *Slc34a2* expression in the kidneys; $r = 0.47$.

592

593 **Figure 3. Immunohistochemistry analysis of *Slc34a2* in freshly harvested rat kidney**
594 **cortex.** Sections of freshly harvested kidneys from a healthy wild-type rat were analysed by
595 immunohistochemistry with anti-*Slc34a2* (*green*) antibody (**this figure**) or the appropriate
596 isotype control (**see Supporting Figure 1**). Cell nuclei were counterstained (*blue*) with
597 Hoescht 33342 and cell cytoskeleton (f-actin, *red*) with phalloidin CF633. Antibody stained

598 sections and isotype controls were collected under identical settings, as stated in Methods. A
599 threshold removing all Slc34a2 attributable signal was defined on the isotype controls and
600 uniformly applied to all images (i.e. antibody stained images). Staining for Slc34a2 within
601 the tubular epithelial cells was distinctly punctate so, as well as the signal above the isotype
602 control being presented in an as-collected 'intensity' format (i.e. the more secondary antibody
603 that is bound, the brighter the signal) (**A & B**), it is also displayed as a binary format (i.e. all
604 signal that is brighter than isotype threshold is given the maximum intensity value) as this
605 aids visualisation (**C & D**). All images are of the kidney cortex and scale-bars are 50 μm . (**B**)
606 As-collected 'intensity' format without actin staining. (**D**) A high power image ($\times 63$
607 magnification) of the area within the quadrant in image (**C**).

608

609 **Figure 4. Fasting urinary phosphorus excretion.** (**a**) Urinary P excretion was measured in
610 the lab chow reference group (Si-high reference; n=6), Si replete (n=5) and Si deplete (n=8)
611 rats by ICP-OES and corrected for creatinine concentration. The higher P excretion in the lab
612 chow reference group is due to the higher P content of the diet (see (**b**)). However, the
613 difference in urinary P excretion between the Si replete and Si deplete rats cannot be
614 explained by a difference in dietary P content, but rather due to the upregulation of Slc34a2
615 in the latter group mediated by Si deficiency in the diet and drinking water (**b**).

616

617 **Figure 5. Transport activity in *RnSlc34a2*-expressing oocytes.** Influx transport activity of
618 *Rattus norvegicus* Slc34a2 for (**a**) arsenate, HAsO_4^{2-} (p= 0.0001), (**b**) phosphate, HPO_4^{2-}
619 (p=0.0008), and (**c**) silicic acid, H_4SiO_4 (p= 0.66). Rice transporter Lsi1 was used as a
620 positive control for H_4SiO_4 influx (p <0.0001). The concentrations of sodium and phosphate
621 in the medium did not influence H_4SiO_4 influx by *RnSlc34a2*-expressing oocytes (**d**), nor that
622 by *OsLsi1*-expressing oocytes (p<0.0001 in both instances). Water-injected oocytes were

623 used as a negative control. In H_4SiO_4 efflux studies **(e)** rice transporter Lsi2 was used as a
624 positive control. Data were corrected against water-injected control oocytes. **(f)** Changes in
625 sodium and phosphate concentration did not affect H_4SiO_4 efflux by Slc34a2 expressing
626 oocytes. Data are shown as means \pm SE (n=15).

627

628 **Figure 6. Germanium transport activity in *RnSlc34a2*-expressing oocytes.** Transport
629 activity for H_4GeO_4 showing **(a)** a lack of influx (p=0.14) but significant efflux **(b)** following
630 a 2 h incubation (p=0.004). Efflux was not significant at 30 minutes (p=0.14) for Slc34a2
631 expressing oocytes. The rice Si transporters Lsi1 and Lsi2 were used as positive controls for
632 influx and efflux activity, respectively (p<0.0001 in both cases compared to negative control,
633 water-injected oocytes).

634

635 **Figure 7. Pairwise alignment of transmembrane domains of Si efflux transporters.**
636 Pairwise alignment of transmembrane domains predicted in *RnSlc34a2* rat protein (*red*) with
637 the four Si efflux transporters in plants (*green*). Transmembrane domains were predicted by
638 OCTOPUS (56) and subsequent alignment was performed by AlignMe tool (51). **(a)** *OsLsi2*
639 (rice) **(b)** *ZmLsi2* (maize), **(c)** *HvLsi2* (barley), **(d)** *CmLsi2-1* (pumpkin).

640

641 **Figure 8. Phylogeny of Slc34a gene family member in vertebrates.** **(a)** The tree was
642 produced using PhyML maximum likelihood analysis with the JTT +G+I model from an
643 alignment of 880 positions. Numbers at nodes are a percentage of 100 bootstrap replicates,
644 with nodes having less than 70% bootstrap support being collapsed. **(b)** The tree was
645 produced using Phylobayes Bayesian MCMC analysis under the CAT +G+I model (15
646 parallel chains with sampling every 100 cycles, burn-in one-fifth the total size of the chain)
647 from an alignment of 880 positions. Numbers at nodes indicate posterior probabilities, with

648 nodes having less than 0.95 support being collapsed. The scale bar indicates the average
649 number of amino acid substitutions per site. The Slc34a1 clade is in green, the Slc34a2 clade
650 in *blue* and the Slc34a3 clade in *red*. The trees are rooted using the single Slc34a homolog
651 identified from the Lamprey genome. The Slc34a gene phylogeny largely agrees with the
652 species phylogeny for vertebrates (33), with incongruent branches (e.g. the basal branches of
653 the a2 clade) only having low statistical support. The maximum likelihood phylogenetic
654 analyses resolve that the Slc34a clade evolved from a single ancestor in jawless vertebrates,
655 and likely involved two main duplication events, initially producing the a3 and a1+2 clades,
656 with a further divergence of the a1 and a2 clades. A teleost-specific duplication event resulted
657 in the evolution of Slc34a2a and Slc34a2b, as found in stickleback and zebrafish. The
658 Bayesian analysis had poor phylogenetic resolution at the base of the a2 clade, but still
659 resolves the a1 and a3 groups as distinct monophyletic clades, and is not incongruous with
660 the maximum likelihood analysis results. For full details of the species and sequences used
661 see Supplemental Table 1.

662

663 **Figure 9. Alignment of vertebrate Slc34a protein sequences showing characteristic motif**
664 **conserved across members of the Slc34a2 group.** The alignment shows the region around
665 the portion identified as unique to rat Slc34a2 in comparison to rat Slc34a1 or a3 (red
666 lettering, see Fig. 1c). Highlighted in yellow are the homologous regions in other vertebrate
667 Slc34a2 proteins, and in the Slc34a-type lamprey sequence. The characteristic Slc34a2 motif
668 identified within this region contains at least three positive residues uninterrupted by any
669 negatively charged residues, with the positive residues regularly spaced apart by at least four
670 small residues (primarily cysteines). A Slc34a sequence containing this motif was found in
671 all vertebrate species investigated. The only members of the Slc34a2 clade (see Fig. 8) where
672 this motif was incomplete was are in the zebrafish and stickleback SLC34a2b (highlighted in

673 *blue*). Positively charged residues are shown in bold and underlined, small amino acids are in
674 italics. Sequence names correspond to the species and gene identifiers given in Supplemental
675 Table 1 and to the phylogeny shown in Fig. 8. The incomplete spiny shark and skate NaPi-IIb
676 sequences are omitted due to this region being missing from the EMBL/Genbank data. The
677 alignment was generated using MUSCLE (<http://www.ebi.ac.uk/Tools/msa/muscle/>).

678 **Table 1. Oxoacid and oxoanion volumes**

	Gas phase	Implicit aqueous solvent
Oxoacid/Oxoanion	V_M (cm ³ /mol)	V_M (cm ³ /mol)
HCO ₃ ⁻	41.9	39.1
H ₃ BO ₃	43.4	43.6
H ₄ BO ₄ ⁻	52.5	55.8
H ₄ SiO ₄	63.2	56.5
H ₄ GeO ₄	61.3	57.8
HPO ₄ ²⁻	62.0	59.2
HAsO ₄ ²⁻	65.0	63.1

679 PBE0/6-31++g(d,p) calculated solvent accessible surface molar volumes (V_M) for various
680 main group oxoacids and oxoanions at physiological pH, showing the similarities between
681 H₄SiO₄, H₄GeO₄ (two oxoacids that are effluxed by Slc34a2), HPO₄²⁻ and HAsO₄²⁻
682 (oxoanions that are influxed by Slc34a2).

683 **Table 2. Predicted transmembrane domains of Slc34a2**

Helices No.	N-terminal	Transmembrane region	C-terminal	Helices type	Length
1	95	FQGIGKFILLGFLYLFVCSLDV	117	1°	23
2	137	NSIMSNPVAGLVIGVLVTVMVQS	159	2°	23
3	166	IIVSMVASSLLSVRAAIIIMGA	188	2°	23
4	374	LILCGCLIMIVKLLGSVLRGQVA	396	1°	23
5	422	VGAGMTFIVQSSSVFTSAMTPLI	444	1°	23
6	459	LGSNIGTTTTAILAALASPGNTL	481	2°	23
7	527	WFAVFYLIFFLLTPLTVFGLSL	549	1°	23
8	555	LVGVGVPILLILLVLCLRMLQA	577	1°	23
9	618	CCCCRVCCRVCCMVCGCKCCRC	640	2°	23

684 The transmembrane domains were predicted using SOSUI software. The sequence
685 highlighted (*yellow*) through multiple sequence alignment of the three *Rattus norvegicus*
686 Slc34 family members (Fig. 1c) is present in the ninth transmembrane helix of Slc34a2. The
687 C-terminal and N-terminal amino acid for each transmembrane domain are indicated, as is
688 the type of alpha-helical structure (i.e. primary or secondary helices, denoted as 1° and 2°
689 respectively).

690 Supplemental Table 1. Sequences used for the vertebrate Slc34a phylogeny

Species Name	Common Name	Gene Name	Accession No.	Notes
<i>Rattus norvegicus</i>	Rat	Slc34a1	gi 6981544	
<i>Rattus norvegicus</i>	Rat	Slc34a2	gi 16758110	
<i>Rattus norvegicus</i>	Rat	Slc34a3	gi 21326473	
<i>Mus musculus</i>	Mouse	Slc34a1	gi 66793411	
<i>Mus musculus</i>	Mouse	Slc34a2	gi 66793411	
<i>Mus musculus</i>	Mouse	Slc34a3	gi 224994177	
<i>Homo sapiens</i>	Human	Slc34a1	gi 156627569	
<i>Homo sapiens</i>	Human	Slc34a2	gi 295789158	
<i>Homo sapiens</i>	Human	Slc34a3	gi 25014088	
<i>Bos taurus</i>	Cow	Slc34a1	gi 157073970	
<i>Bos taurus</i>	Cow	Slc34a2	gi 27807195	
<i>Bos taurus</i>	Cow	Slc34a3	gi 528970641	
<i>Loxodonta africana</i>	Elephant	Slc34a1	gi 344265327	
<i>Loxodonta africana</i>	Elephant	Slc34a2	gi 344298758	
<i>Loxodonta africana</i>	Elephant	Slc34a3	gi 344309900	
<i>Monodelphis domestica</i>	Opossum	Slc34a1	gi 126291054	
<i>Monodelphis domestica</i>	Opossum	Slc34a2	gi 126331900	
<i>Monodelphis domestica</i>	Opossum	Slc34a3	gi 126302869	
<i>Ornithorhynchus anatinus</i>	Platypus	Slc34a1	gi 149423843	
<i>Ornithorhynchus anatinus</i>	Platypus	Slc34a2	gi 345307737	
<i>Anolis carolinensis</i>	Lizard	Slc34a1	gi 327265671	
<i>Anolis carolinensis</i>	Lizard	Slc34a2	gi 327282884	
<i>Gallus gallus</i>	Chicken	Slc34a1	gi 513206663	
<i>Gallus gallus</i>	Chicken	Slc34a2	gi 46048932	
<i>Xenopus tropicalis</i>	Frog	Slc34a2	gi 46195785	Multiple hits, several duplicates or redundant sequences
<i>Xenopus tropicalis</i>	Frog	Slc34a3	gi 301622941	Multiple hits, several duplicates or redundant sequences
<i>Latimeria chalumnae</i>	Coelacanth	Slc34a2	ENSLACP00000002539	Genome not yet searchable within EMBL/Genbank database
<i>Latimeria chalumnae</i>	Coelacanth	Slc34a3	ENSLACP00000014496	Genome not yet searchable within EMBL/Genbank database
<i>Takifugu rubripes</i>	Pufferfish	Slc34a1	gi 410915152	
<i>Takifugu rubripes</i>	Pufferfish	Slc34a2	gi 410920832	
<i>Danio rerio</i>	Zebrafish	Slc34a2	gi 33504533	
<i>Danio rerio</i>	Zebrafish	SLC34 2a	gi 18859377	
<i>Squalus acanthias</i>	Spiny Shark	NaPi-IIb1	gi 11494391	No genome available, Single sequence deposit, not full length transcript
<i>Squalus acanthias</i>	Spiny Shark	NaPi-IIb2	gi 11494393	No genome available, Single sequence deposit, not full length transcript
<i>Callorhynchus milii</i>	Elephant Shark	SLC34a	AAVX01126234.1	Draft genome, not yet searchable within EMBL/Genbank database, not full length transcript
<i>Leucoraja erinacea</i>	Skate	NaPi-IIb1	gi 11494395	No genome available, Single sequence deposit, not full length transcript
<i>Leucoraja erinacea</i>	Skate	NaPi-IIb2	gi 11494399	No genome available, Single sequence deposit, not full length transcript
<i>Petromyzon marinus</i>	Lamprey	SLC34A	ENSPMAP00000003321	Genome not yet searchable within EMBL/Genbank database

691 The Slc34a sequences were selected on the basis of taxonomic coverage of relevant
692 vertebrate groups, availability of fully sequenced genomes and sequence completeness and
693 homology to rat Slc34a genes. Where multiple homologs were recovered from the same
694 genome project, the sequences were inspected to remove any duplicated or erroneous
695 sequences. Taxonomic classifications are based on the EMBL/Genbank or genome
696 sequencing project annotations as relevant. The common names shown are used in the Slc34a
697 phylogeny in Fig. 8. Gene names are given according to the relevant BLASTp or tBLASTn
698 hit to rat Slc34a1, a2 or a3. In cases where the sequences were recovered from incompletely
699 sequenced genomes or where the homology was unclear a more general gene name
700 classification was used. In the case of the Spiny Shark and Skate sequences the gene names
701 were taken directly from the EMBL/Genbank annotations and refer to "Type II Sodium-
702 Phosphate co-transporter", a synonym of Slc34a.

703

04 **Supplemental Table 2. Modified Barth's solutions**

05	(i)	Modified Barth's Saline (MBS) solution											Osm		
		Na ⁺	Cl ⁻	NO ₃ ⁻	K ⁺	Ca ²⁺	Mg ²⁺	HPO ₄ ²⁻	SO ₄ ²⁻	HCO ₃ ⁻	HEPES				
		(mM)	(mM)	(mM)	(mM)	(mM)	(mM)	(mM)	(mM)	(mM)	(mM)	(mM)	(mmol/L)		
	NaCl	82	82	82									164		
	KCl	1		1	1								2		
	Ca(NO ₃) ₂	0.33		0.66		0.33							0.99		
	CaCl ₂	0.41		0.82		0.41							1.23		
	MgSO ₄	0.82					0.82		0.82				1.64		
	NaHCO ₃	2.4	2.4							2.4			4.8		
	Na HEPES	10	10								10		20		
	Osm (mmol/L)		94.4	83.82	0.66	1	0.74	0.82	0	0.82	2.4	10	195		
06	HEPES (4-(2-hydroxyethyl)-1-piperazineethanesulfonic acid); Osm (osmolarity)														
07	(ii)	MBS1 (MBS supplemented with 1.7 mM H ₄ SiO ₄)											Osm		
		Na ⁺	Cl ⁻	Rb ⁺	Ca ²⁺	Mg ²⁺	HPO ₄ ²⁻	SO ₄ ²⁻	HEPES	HCO ₃ ⁻	NO ₃ ⁻	Si(OH) ₄			
		(mM)	(mM)	(mM)	(mM)	(mM)	(mM)	(mM)	(mM)	(mM)	(mM)	(mM)	(mmol/L)		
	NaCl	82	82	82									164		
	RbCl	1		1	1								2		
	Ca(NO ₃) ₂	0.33			0.3						0.7		1		
	CaCl ₂	0.41		0.8	0.4								1.2		
	Na HEPES	10							5				5		
	MgSO ₄	0.82				5		5					10		
	NaHCO ₃	2.4	5							5			10		
	Na ₂ O ₃ Si	1.7	4									2	6		
	Osm (mmol/L)		91	83.82	1	0.74	5	0	5	5	5	0.66	2	199	
08	HEPES (4-(2-hydroxyethyl)-1-piperazineethanesulfonic acid); Osm (osmolarity)														
09	(iii)	MBS2 (1.7 mM H ₄ SiO ₄ , 10 mM Na ⁺ & 0.5 mM HPO ₄ ²⁻)													Osm
		Na ⁺	Cl ⁻	NO ₃ ⁻	NMG	K ⁺	Ca ²⁺	Mg ²⁺	HPO ₄ ²⁻	SO ₄ ²⁻	HCO ₃ ⁻	HEPES	Si(OH) ₄	Glu	
		(mM)	(mM)	(mM)	(mM)	(mM)	(mM)	(mM)	(mM)	(mM)	(mM)	(mM)	(mM)	(mM)	(mmol/L)
	NMG-Cl pH 7.4	74		74	74										148
	NaCl	6	6	6											12
	KCl	1		1		1									2
	Ca(NO ₃) ₂	0.33		0.66			0.33								0.99
	CaCl ₂	0.41		0.82			0.41								1.23
	NMG HPO ₄	0.5			0.5			0.5							1
	NMG HEPES	15			15						15				30
	MgSO ₄	0.82					0.82		0.82						1.64
	Na ₂ O ₃ Si	1.7	4										2		6
	Ouabain	0.1													
	NMG gluconate	1.5			1.5									1.5	3
	Osm (mmol/L)		10	81.82	0.66	91	1	0.74	0.82	0.5	0.82	15	2	1.5	206
10	NMG (N-methyl-D-glucamine); HEPES (4-(2-hydroxyethyl)-1-piperazineethanesulfonic acid); Osm (osmolarity); Glu (gluconate)														

11 (iv) MBS3 (0 mM Na⁺ & 0 mM HPO₄²⁻)

	Na ⁺ (mM)	Cl ⁻ (mM)	NO ₃ ⁻ (mM)	K ⁺ (mM)	Ca ²⁺ (mM)	Mg ²⁺ (mM)	HPO ₄ ²⁻ (mM)	SO ₄ ²⁻ (mM)	HCO ₃ ⁻ (mM)	HEPES (mM)	Osm (mmol/L)
NMG-Cl pH 7,4	80	80									160
KCl	1	1		1							2
Ca(NO ₃) ₂	0.33		0.66		0.33						0.99
CaCl ₂	0.41	0.82			0.41						1.23
NMG HEPES	15									15	30
MgSO ₄	0.82					0.82		0.82			1.64
Osm (mmol/L)	0	81.82	0.66	1	0.74	0.82	0	0.82	0	15	196

12 NMG (N-methyl-D-glucamine); HEPES (4-(2-hydroxyethyl)-1-piperazineethanesulfonic acid); Osm (osmolarity)

13

14

15 (v) MBS4 (10 mM Na⁺, 0.5 mM HPO₄²⁻)

	Na ⁺ (mM)	Cl ⁻ (mM)	NO ₃ ⁻ (mM)	NMG (mM)	K ⁺ (mM)	Ca ²⁺ (mM)	Mg ²⁺ (mM)	HPO ₄ ²⁻ (mM)	SO ₄ ²⁻ (mM)	HEPES (mM)	Glu (mM)	Osm (mmol/L)
NMG-Cl pH 7,4	74	74		74								148
NaCl	6	6										12
KCl	1	1			1							2
Ca(NO ₃) ₂	0.33		0.66			0.33						0.99
CaCl ₂	0.41	0.82				0.41						1.23
NMG HPO ₄	0.5			0.5				0.5				1
NMG HEPES	15			15						15		30
MgSO ₄	0.82						0.82		0.82			1.64
Ouabain	0.1											
NAG gluconate	4	4									4	8
Osm (mmol/L)	10	81.82	0.66	89.5	1	0.74	0.82	0.5	0.82	15	4	205

16 NMG (N-methyl-D-glucamine); HEPES [4-(2-hydroxyethyl)-1-piperazineethanesulfonic acid]; Osm (osmolarity); Glu (gluconate)

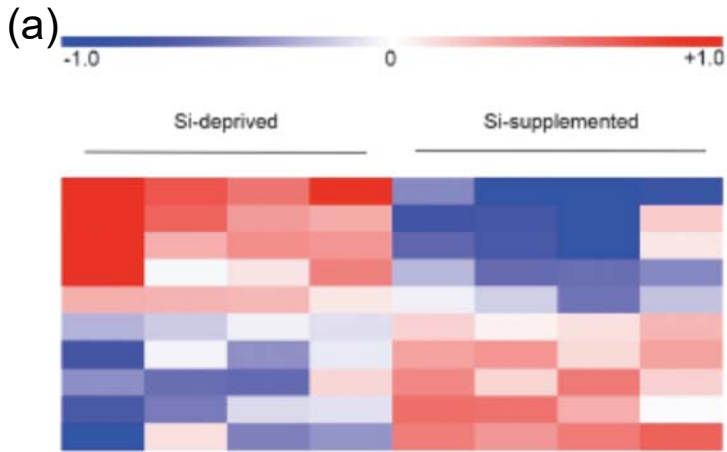
17

18

19 (vi) MBS5: 84 mM Na⁺ & 2 mM HPO₄²⁻

	Na ⁺ (mM)	Cl ⁻ (mM)	NO ₃ ⁻ (mM)	NMG (mM)	K ⁺ (mM)	Ca ²⁺ (mM)	Mg ²⁺ (mM)	HPO ₄ ²⁻ (mM)	SO ₄ ²⁻ (mM)	HCO ₃ ⁻ (mM)	HEPES (mM)	Glu (mM)	Osm (mmol/L)
NaCl	80	80											160
KCl	1	1			1								2
Ca(NO ₃) ₂	0.33		0.66			0.33							0.99
CaCl ₂	0.41	0.82				0.41							1.23
NMG HPO ₄	2			2				2					4
NMG HEPES	15			15							15		30
MgSO ₄	0.82						0.82		0.82				1.64
Ouabain	0.1												
NAG gluconate	4	4										4	8
Osm (mmol/L)	84	81.82	0.66	17	1	0.74	0.82	2	0.82	0	15	4	208

20 NMG (N-methyl-D-glucamine); HEPES [4-(2-hydroxyethyl)-1-piperazineethanesulfonic acid]; Osm (osmolarity); Glu (gluconate)

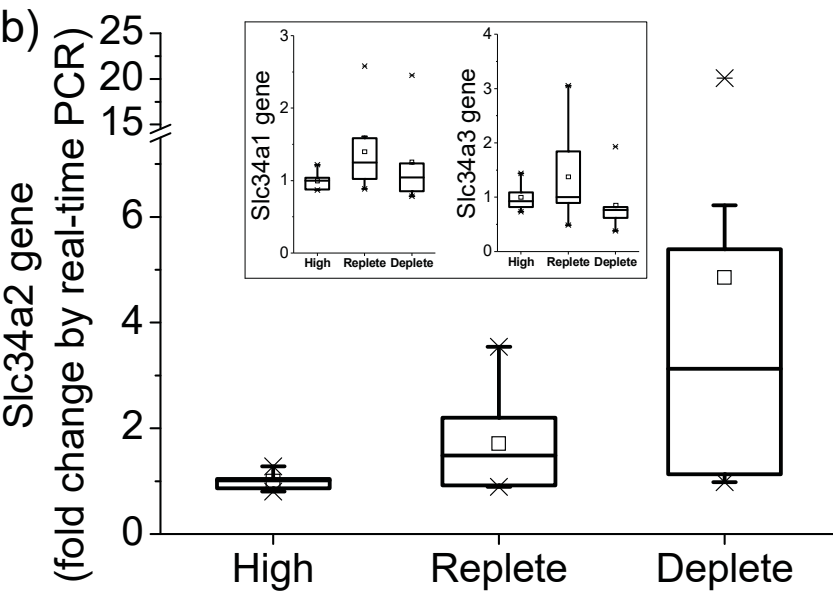


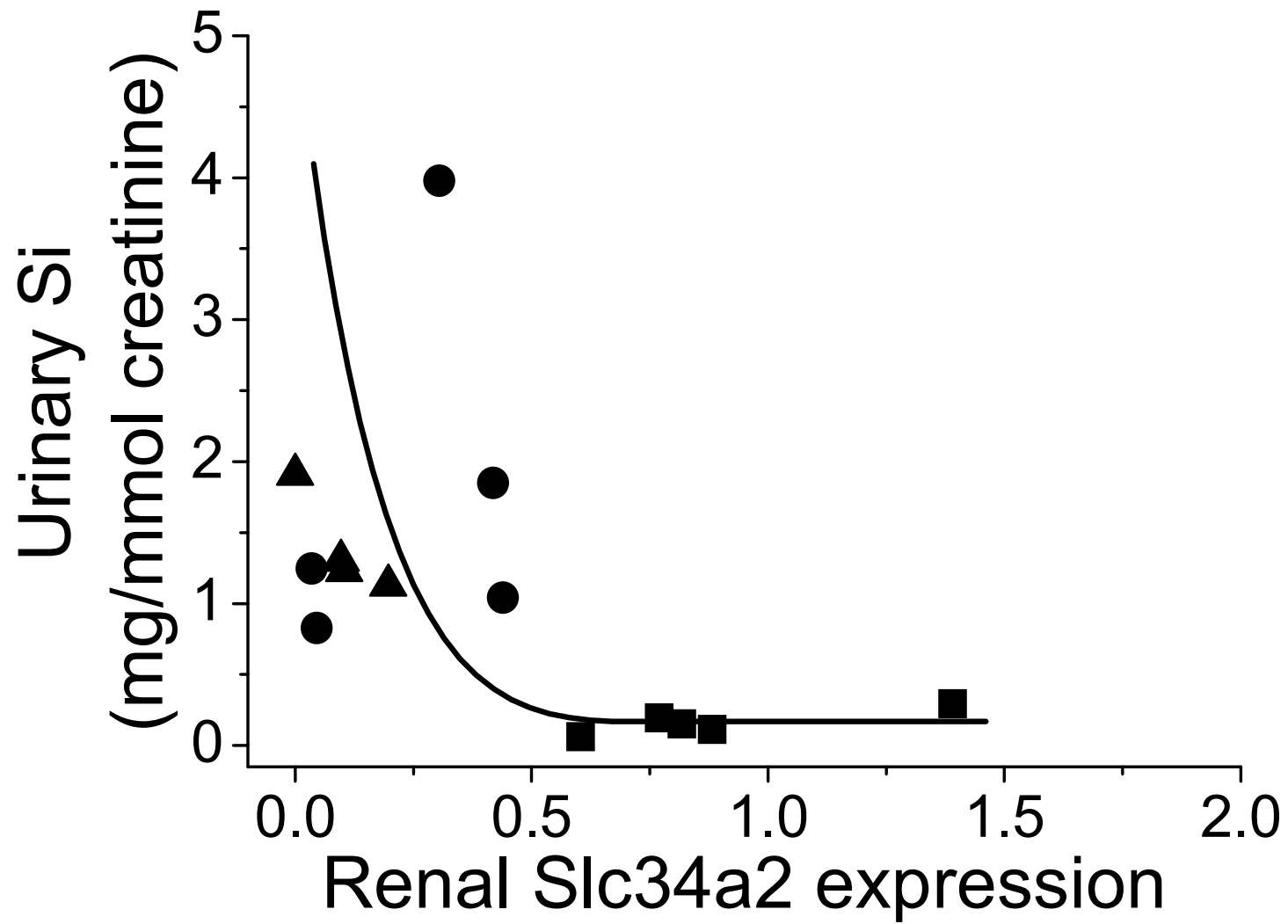
(c) Multiple sequence alignments for Slc34a2, Slc34a1, and Slc34a3. Conserved residues are indicated by asterisks (*). Conserved blocks are indicated by double asterisks (**).

```

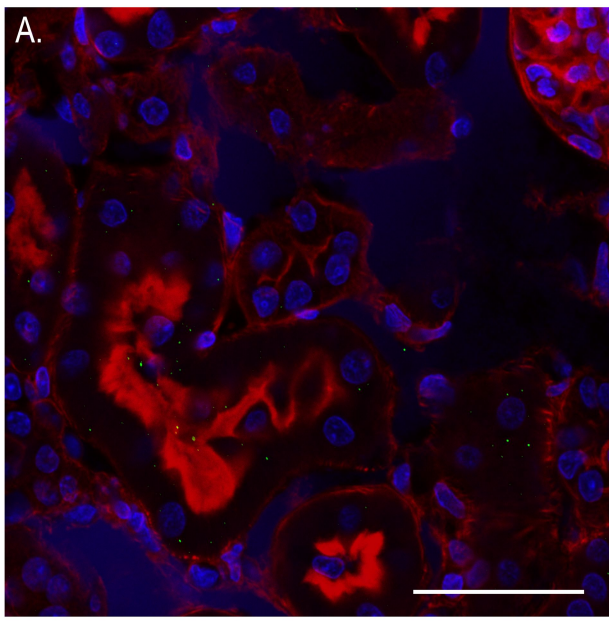
Slc34a2| MAPWPELENA---HPNPNK---FIEGASG---PQSSIPDKDKG-TSKTNDSTGTPVAKIEL
Slc34a1| MMSYSERLGGPAVSPPLVVRGRHMVHGAAFAVVPSPQVLHRIPTGTYAISLSPVALTEH
Slc34a3| M---PNSLAGDQ--VPNPITLD---AIGLVDWLSLRNAGTSGSTPG-----
*      *      *      *      *      *      *      *      *      *
Slc34a2| LPSYSALVLIIEEPPGNDPDPQLDNGIKWSEKSKGKILCFQIGIKFILLGFLYL
Slc34a1| SCPYGEVL-----ECHDPLPAKLAQEEEQKPEPRLSQ-KLAQVGTLLKVLMLGFLYL
Slc34a3| -----LEEG--GTDPTWFSQLKNTDQKKEVGTAS-KLHQVVSGLKACGLLGSLYF
**      *      *      *      *      *      *      *      *      *
Slc34a2| FVCSLDVLSAFPQLVGGKMGQFFSNNSIMSNPVAGLVIGVLTVMVQSSSTSSSIIVSM
Slc34a1| FVCSLDVLSAFPQLVGGKMGQFFSNNSIMSNPVAGLVIGVLTVMVQSSSTSSSIIVSM
Slc34a3| FICSLDILLSAFPQLLGGKMGQFFSNNSIMSNPVAGLVIGVLTVMVQSSSTSSSIIVSM
*****
Slc34a2| VASSLLSVRAAIPIMGANGITSTINTIVALMQAGDRNEFRRAFAGATVHDFFNWLSVLV
Slc34a1| VSSGLEVSSAIPIMGANGITSTINTIVALMQAGDRDFRRRAFAGATVHDFCNWLSVLV
Slc34a3| VASKSLTVQASVPIMGVNVGTSITSTLVMSAQSGDRDFQRAFGGSAVHGIFNWLTVLV
* * * * *
Slc34a2| LLPLEAATHYLEKLTNLVLETFSFQNGEDAPDILKVITDPFTKLIQLDKKVIQIQIAMGD
Slc34a1| LLPLEAATGYLHHVTGLVVASFNIRGGRDAPDLKVIETFPFTKLIQLDKSVVTSIAVGD
Slc34a3| LLPLENATAALERLSELALGAASLPQGGQAPDILKALTRPFTHLIIQLDSSVVTSSITSN
*****
Slc34a2| SEAQNKSLIKIWCKTISNVIEENVTVPSPDNCTSPSYCWTDGIQWTWITQNVTEKENIAKC
Slc34a1| ESLRNHSLIRIWCQP-----ETKEASTSMSRVEAIG---SLANTT---MEKC
Slc34a3| TT--NSSLIKHWCGFRG-----ETPQG--SSECDLGSSTERNSSASPGEDRLLC
* * * * *
Slc34a2| QHIFVNFSLPDLAVGILLTVSLLILCGCLIMIVKLLGSVLRGQVATVIKKTINTDFPFP
Slc34a1| NHIFVDTGLPDLAVGLLAGSLVVLCTCLILLVLMKLSLLKGGVANVIQKVINTDFPAP
Slc34a3| HHLFAGSELTDLAVGILLLAGSLLVLCVCLVIVKLLNSVLRGRIAQAVKTVINADFPFP
* * * * *
Slc34a2| FAWLTGYLAILVAGMTFIVQSSSVFTSAMTPILIGVISIERAYPLTLGNSIGTTTTAI
Slc34a1| FTWVTGYFAMVVGASMTFVQSSSVFTSAITPLILGLGVI SIERAYPLTLGNSIGTTTTAI
Slc34a3| FGWLSGYLAILVAGLTFLLQSSSVFTAIVPLMGVGVINLERAYPLFLGNSIGTTTTAL
* * * * *
Slc34a2| LAALASPGNTRSSQLIALCHFFFNISGILLWYPIPFTRLP IRLAKGLNISAKYRWFVA
Slc34a1| LAALASPREKLSFFQIALCHFFFNISGILLWYPLPCTRLP IIRMAKALGKRTAKYRWFVA
Slc34a3| LAALASPADTLLFAVQVALIHFFFNLAGILLWYLVPLRLPI PLAKRFGDLTAQYRWVAI
*****
Slc34a2| FYLIFPFLTPTLVFGLSLAGWPVLVGVGVPILLIILLVLCRLMLQARCPRI LPLKLRDW
Slc34a1| LYLLVCFLLLPVLFVGMAGWQAMVGVTPFGALLAFVVLVNLQSRSPGHLPKWLQW
Slc34a3| VYLLLTFLLLPLAAGFLSLAGGSVLAAVGGPLVGLVLLI ILVNVLQRRHRSWLPRLQSW
** * * * *
Slc34a2| NFLPLWMHSLKPWDNIISLATSCFQRCCCCCRVCCRCVCCGCKCCRCCKCNLEEE
Slc34a1| DFLPRWMSLQPLDGLITRATLCYAR-----
Slc34a3| AWLPLWLHSLPWRDLVT-----GCC-----
* * * * *
Slc34a2| EKEQDVPVKASGGFDNTAMSKECQDEGKQVEVLGMKALSNTTVF
Slc34a1| PRSPQLPPRV-----FLEELPATPSPR--LALPAHNNATRL
Slc34a3| -----PFKA---YNSNHMTSKVAHCYENPQ--VIASQQL-----
*

```

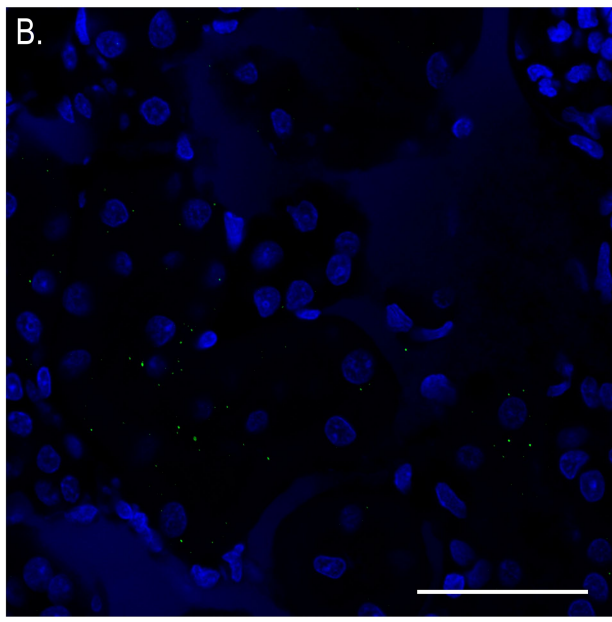




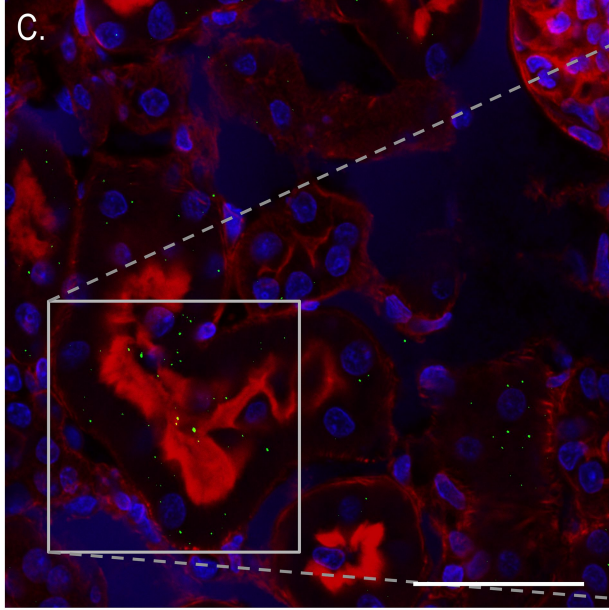
Nuclei / Actin / SLC34A2 (intensity)



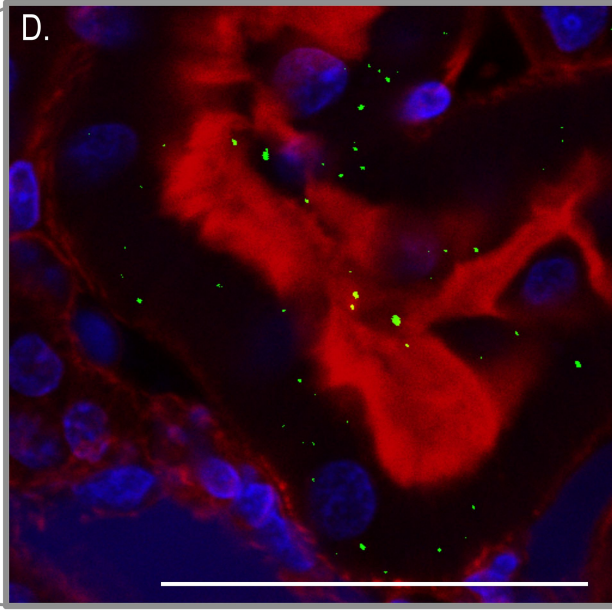
Nuclei / SLC34A2 (intensity)

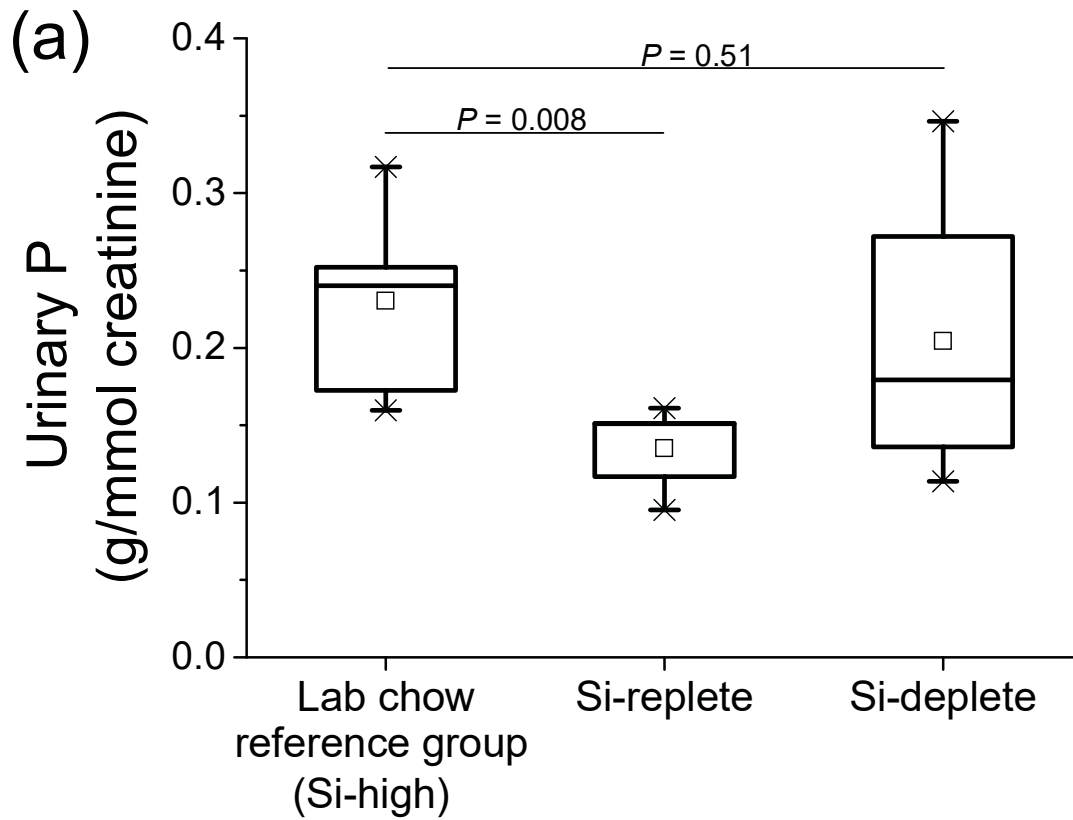


Nuclei / Actin / SLC34A2 (binary)



Inset: Nuclei / Actin / SLC34A2 (binary)

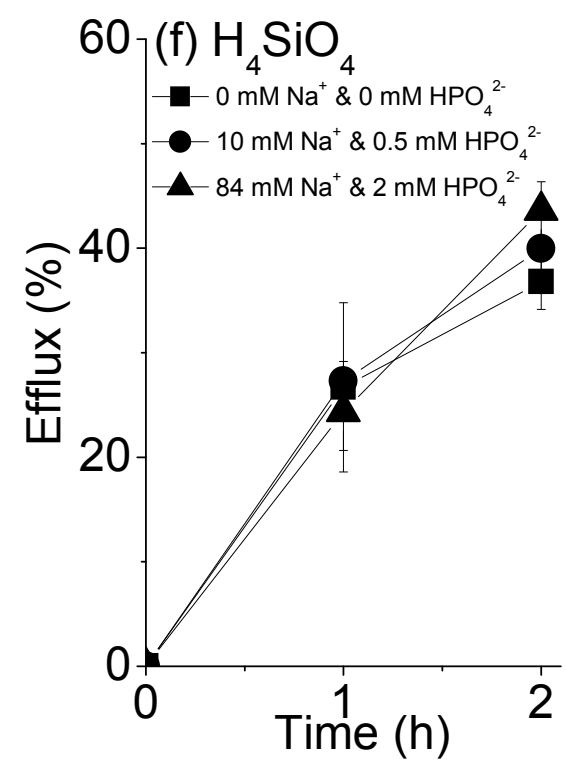
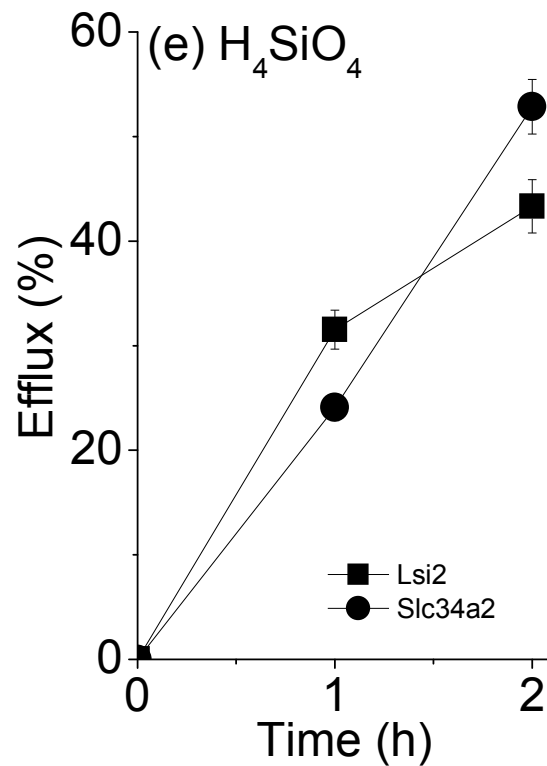
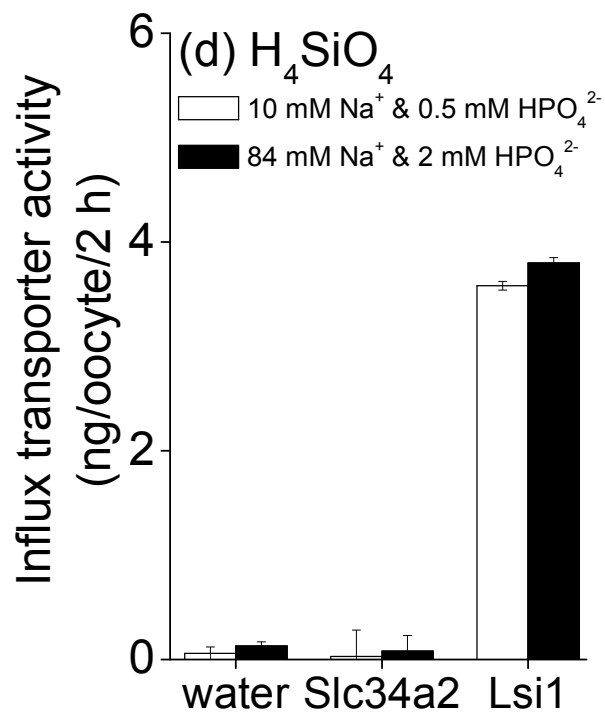
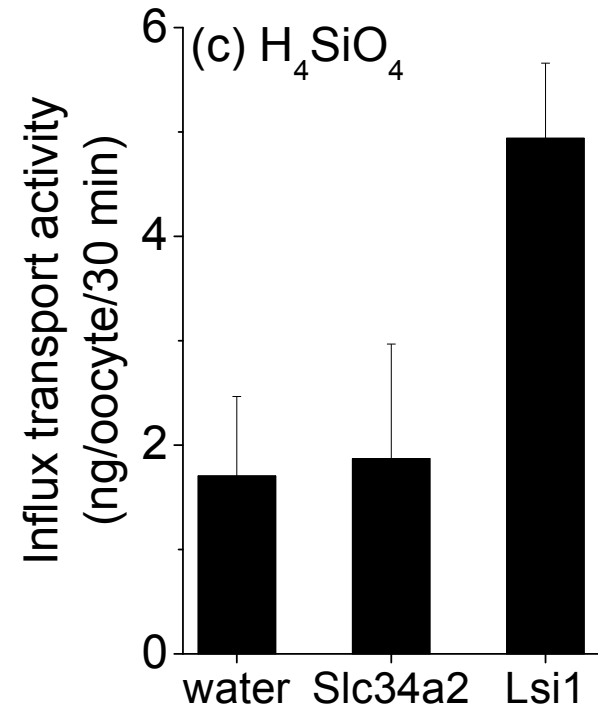
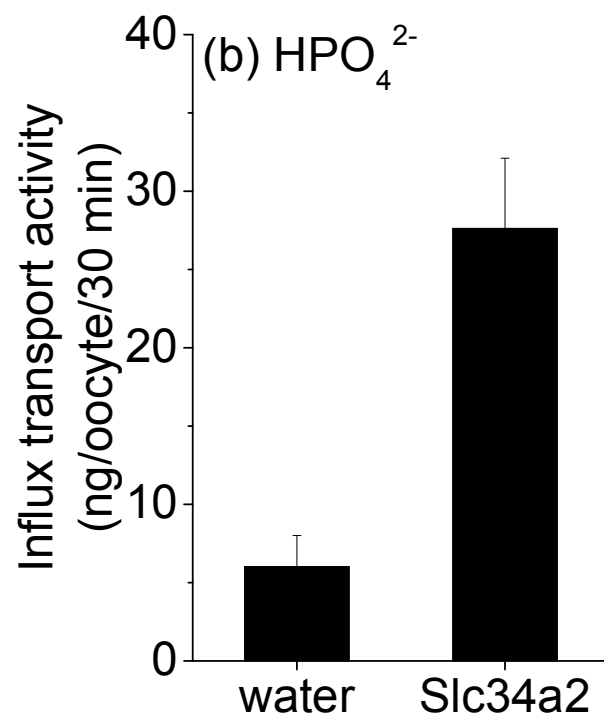
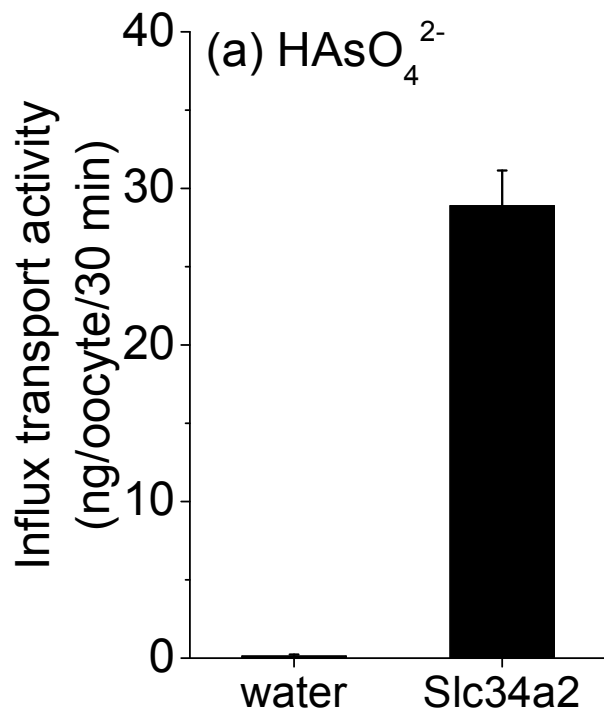


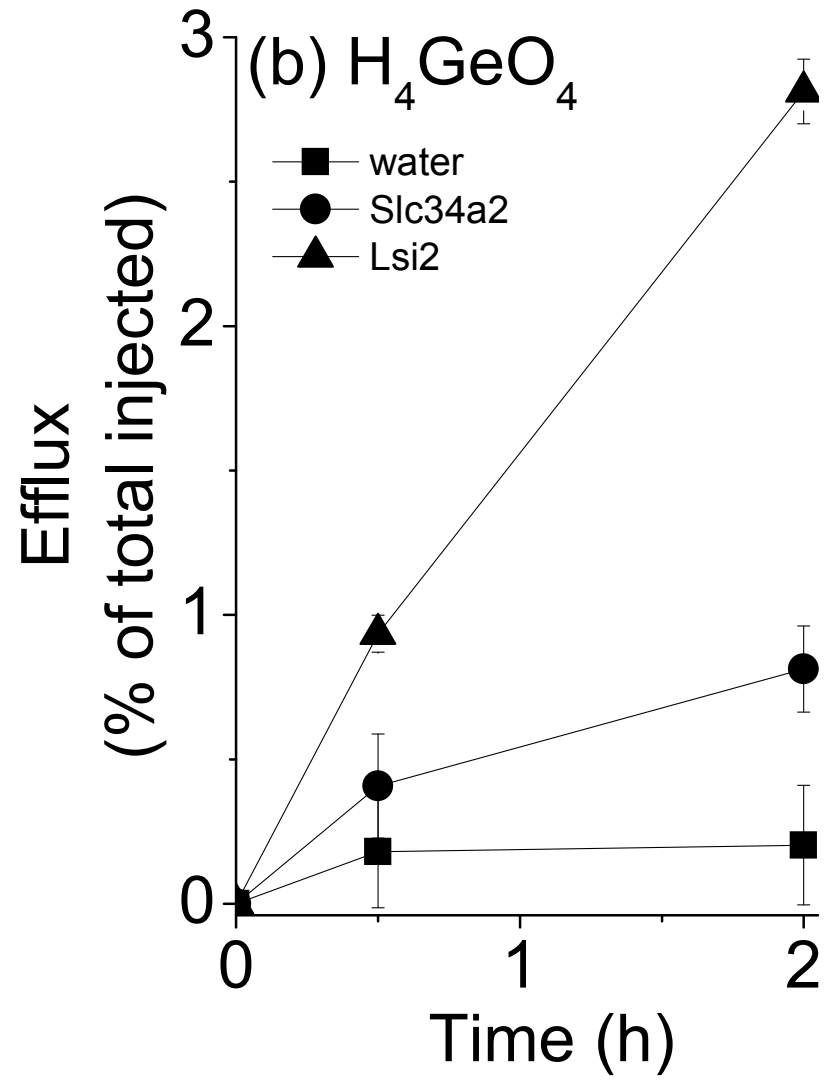
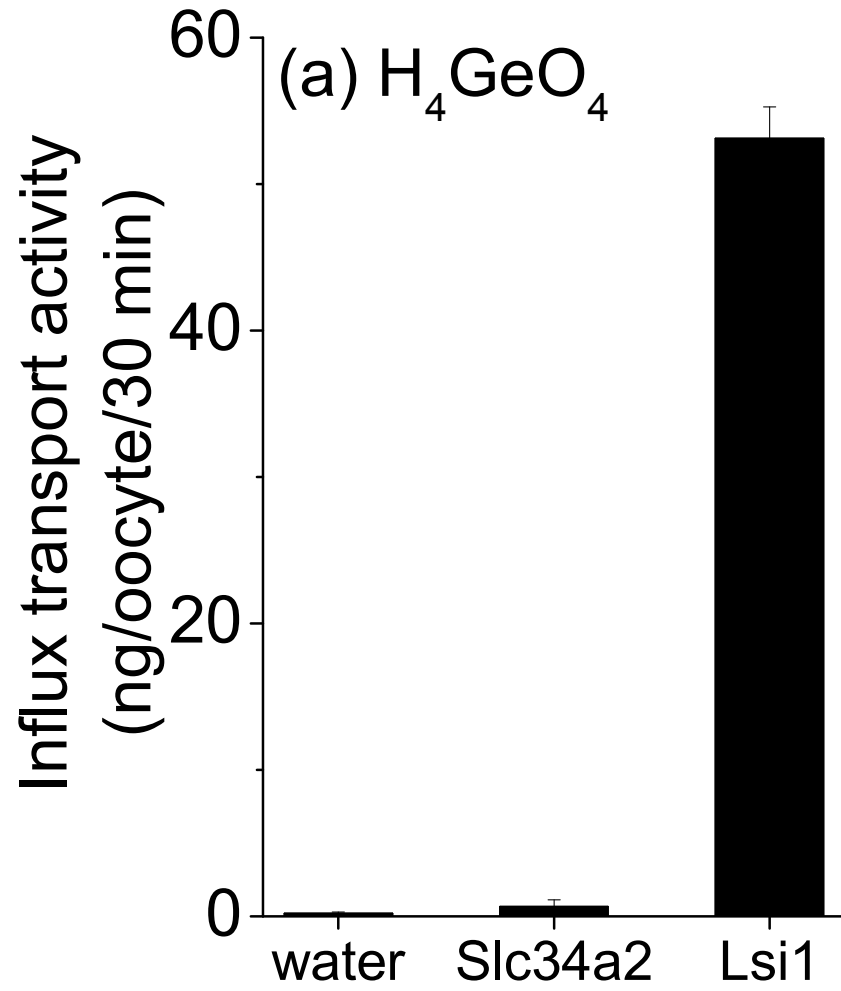


(b)

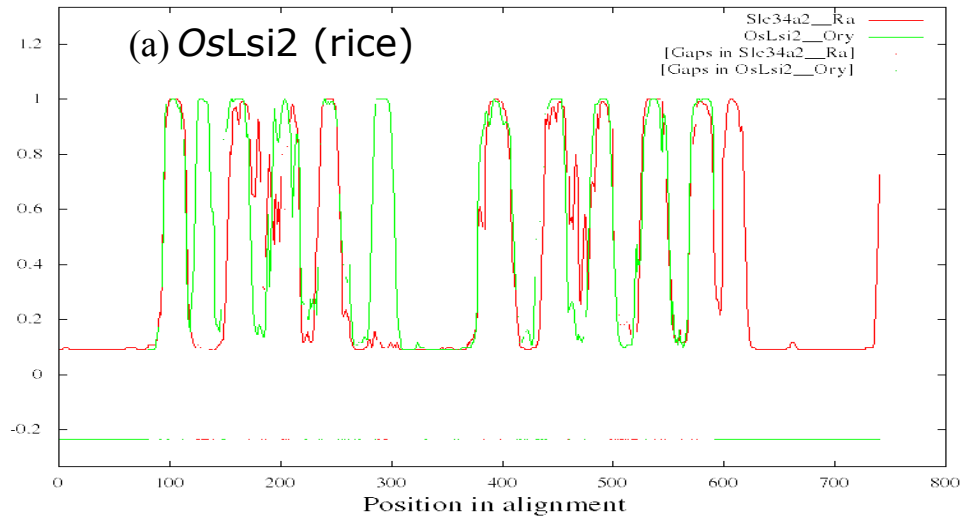
	Lab chow reference group (Si-high)	Si -replete	Si-deplete
Renal Slc34a2 (relative expression)*	0.336 ± 0.062	0.574 ± 0.308	1.63 ± 1.90
Si (µg/g feed)	322 ± 47	3.2 ± 0.6	3.2 ± 0.6
Si (µg/g drinking water)	5.04 ± 1.12	53.2 ± 0.6	0.015 ± 0.010
P (g/kg feed)	7.00	2.28	2.28

*Summarised from Figure 1b

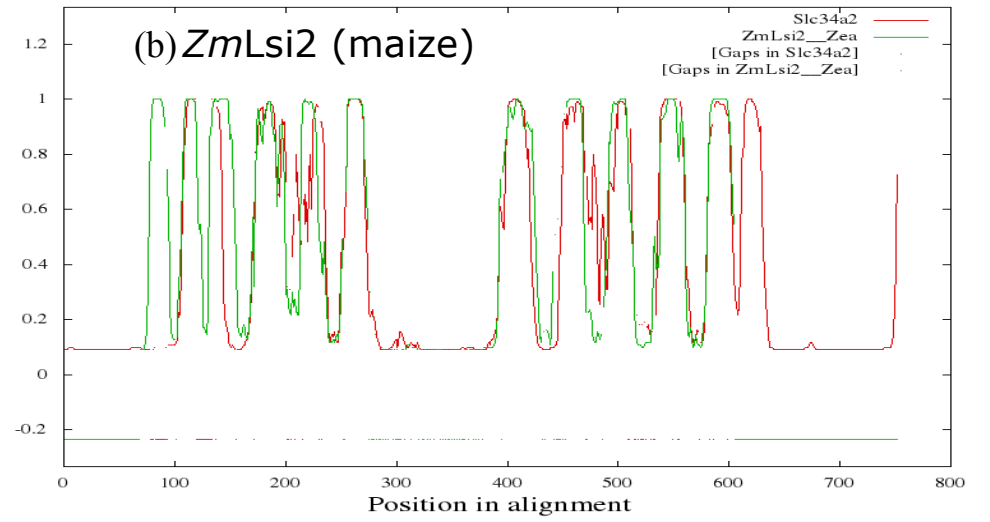




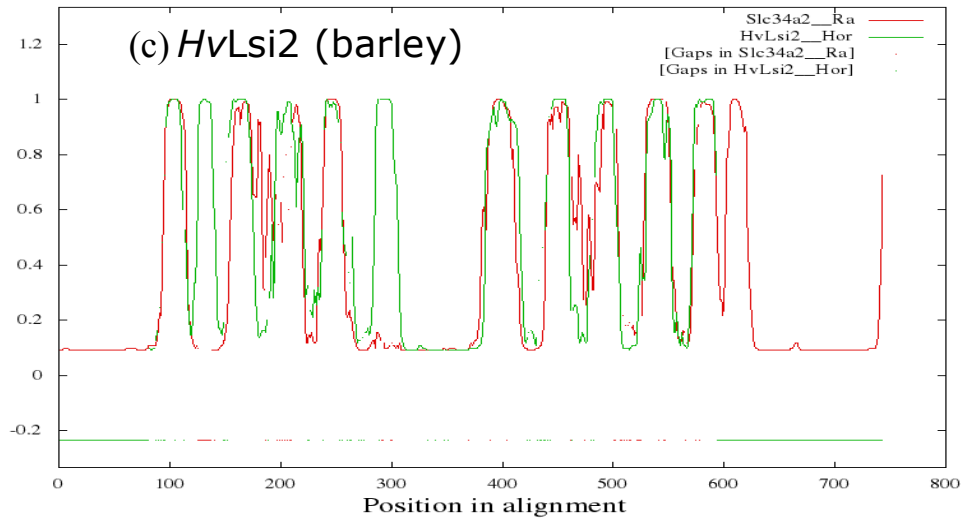
Membrane probabilities obtained with OCTOPUS



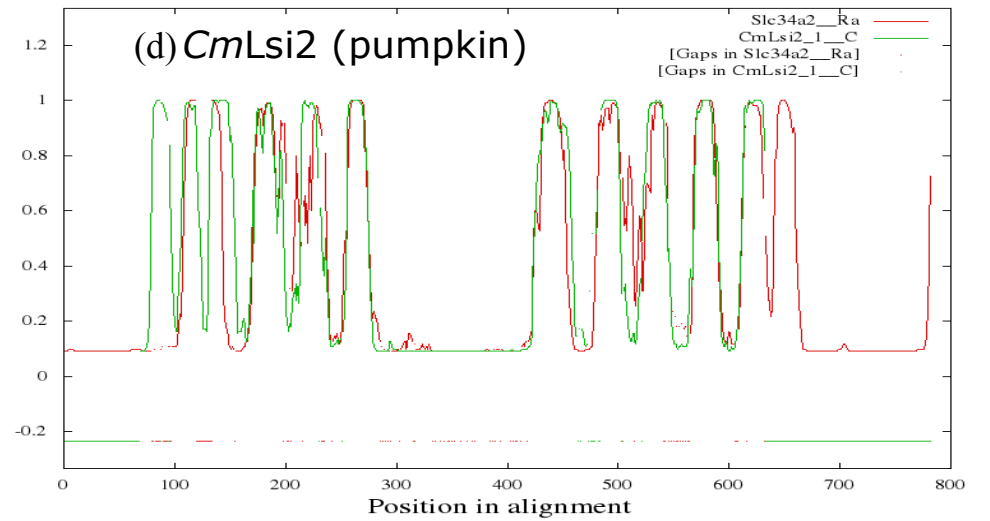
Membrane probabilities obtained with OCTOPUS

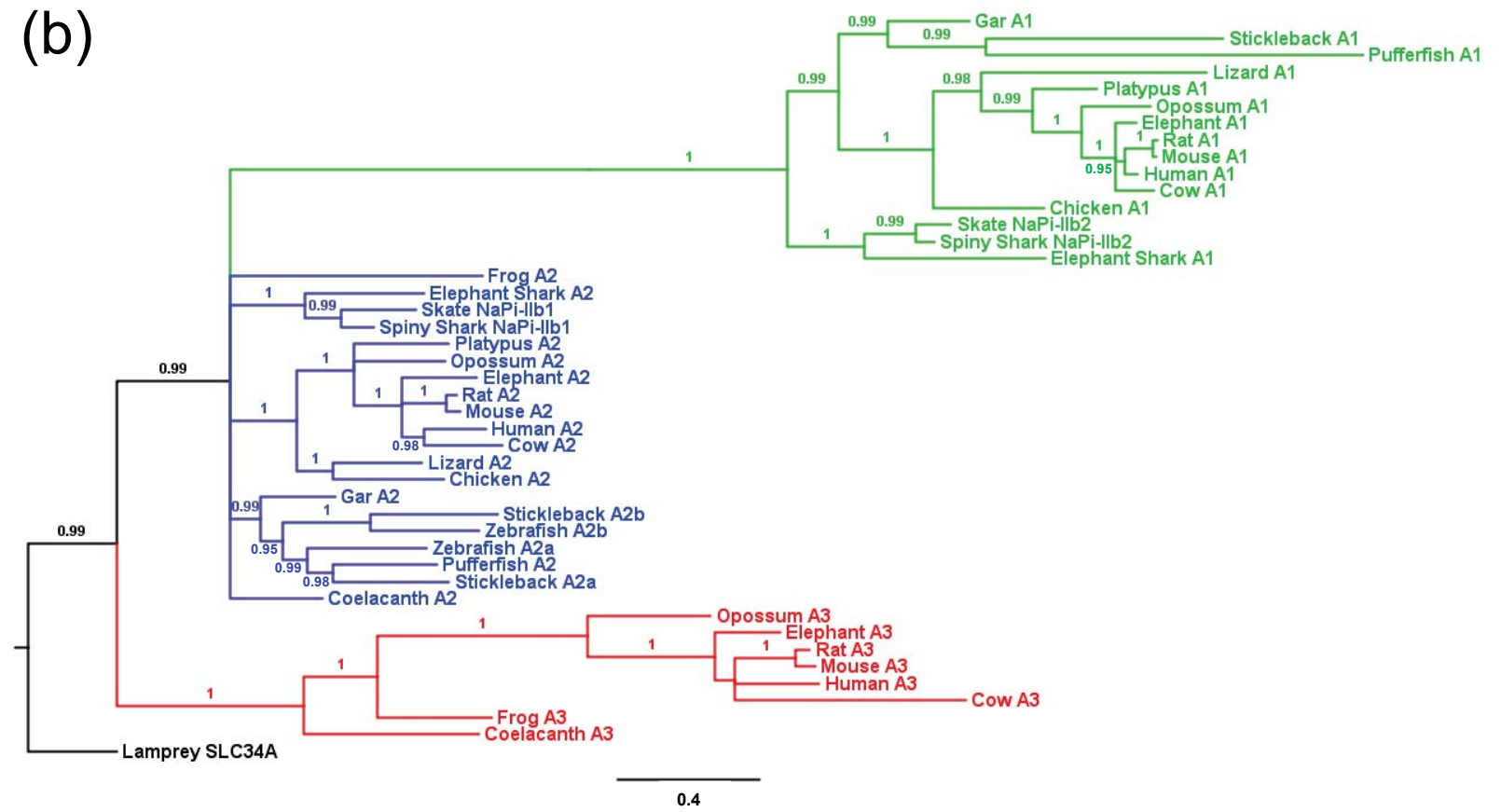
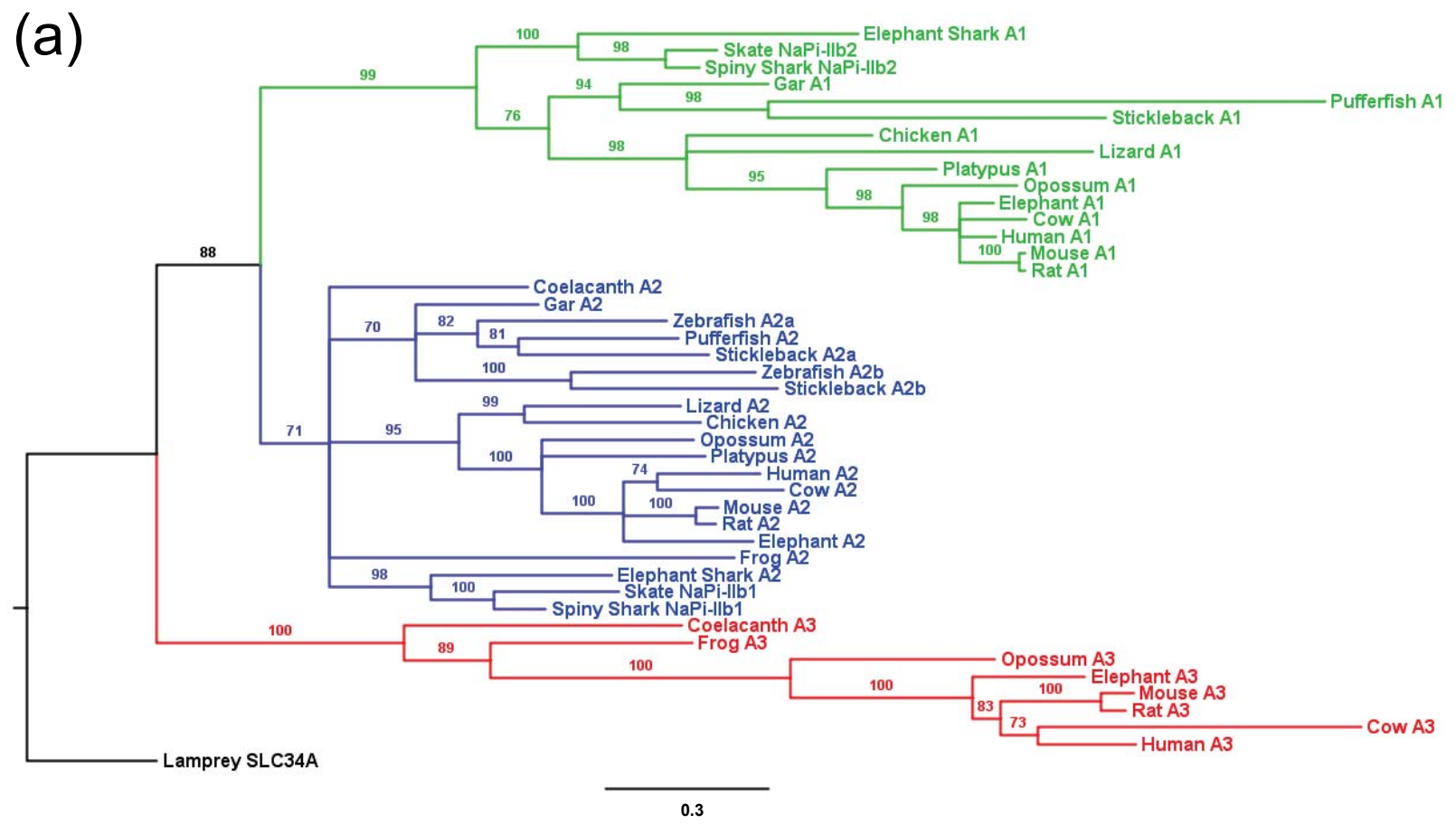


Membrane probabilities obtained with OCTOPUS



Membrane probabilities obtained with OCTOPUS





Pufferfish Slc34a1	NWDFFPWMTSLQPIDDLITRMS-----RVCQRNRRGWRI--HRNRSTTFLERGTVHTVTN
Stickleback Slc34a1	SWDFLPKWMRSLKPLDRLITKATA-----CGCS-----GHQDARGEDGGDGRMSTKEIVRESAQKME----QL
Lizard Slc34a1	SWDFLPFWLRSLQPM DGLITRTRM-----CCTV-----CCSYSREKHSATSPQMKAKLGLCNPSLSFLGELSPPKPS
Gar Slc34a1	SWDFLPWGMHSLKPM DAFITNATL-----CCTV-----HCSTKNSDVQGGPVSFSDSFAEKKAKMA-----
Elephant Shark Slc34a1	NWDFLPIWMHSLKPM DRVITNVTL-----YCT-----NHCRSEKTDLKEVNCQQERSPQLKEK-----AV
Chicken Slc34a1	SWDFLPWMMHSLQPLDSLITRATL-----CCT-----DRCRSPGEGWD---EREAAARDKARLGLDNPVL
Opossum Slc34a1	TWDFLPYWMHSLKPLDRLITRATL-----CCTH-----PEPRSPPLPTRVYLEELPTATPSPRLGVLPDDT
Platypus Slc34a1	TWEFLPRWMRSLKPLDGLITRATL-----CCAH-----ADPAKSPRLPARATYDNP GARVYLQEL----PR
Cow Slc34a1	TWDFLPLWMHSLKPLDRLITRATL-----CCAR-----AEPRSPPLPARVFLLEELPPATPSPHLA-----
Mouse Slc34a1	TWDFLPRWMHSLQPLDGLITRATL-----CYAR-----PEPRSPQLPPRVFLEELPPATPSPRLA-----
Rat Slc34a1	TWDFLPRWMHSLQPLDGLITRATL-----CYAR-----PEPRSPQLPPRVFLEELPPATPSPRLA-----
Elephant Slc34a1	TWDFLPQWMHSLKPLDHFITRATL-----CCAR-----PEPRSPMPRRVFLLEELPPATPSPHLA-----
Human Slc34a1	TWDFLPRWMHSLKPLDHLITRATL-----CCAR-----PEPRSPPLPPRVFLEELPPATPSPRLA-----
Frog Slc34a2	NWDFLPKWMHSLKPWDSCMGASL-LCR HFCCCC ----- CGKMCKPKCKCKCH DK-----EDEEYSIEPKQA----LE
Platypus Slc34a2	NWDFLPKWMHSLKPWDVSVSGLTG-SFR KCCCC ----- RICMCLCGCPPCCRCCKCR DSGTEDEEPKADIPVKG----GE
Opossum Slc34a2	NWHFLPLWMRSLQPWDGIVSLLTGNCCQLPCCWCC RACCRVCCLLCGCFRCCRC SKCCDLL---EEEEENVKEIPIKV----PE
Cow Slc34a2	SWDFLPFWMRSLPDKLITSLTS-CFQM RCCCCRVCCRLCCGLCGCSKCCRC TCS-----EDLEEGKDEPVKS----PE
Elephant Slc34a2	NWNFLPLWMHSLKPWDHLISLTS-CCQ RCCCC --- CCHLCCVLCGCFKCCRCNK YLEDL-EEGQEYSKDTPIKT----PN
Human Slc34a2	NWNFLPLWMRSLKPWDVAVSKFTG-CFQM RCCCCRVCCRACCLLCGCFKCCRC SKCCEDL---EEAQEGQDVPVKA----PE
Mouse Slc34a2	DWNFLPLWMHSLKPWDNVI SLATT-CFQR RCCCCRVCCRVCCMVCGC-KCCRC SKCCRDQGE EEEEEKEQDIPVKA----SG
Rat Slc34a2	DWNFLPLWMHSLKPWDNIISLATS-CFQR RCCCCRVCCRVCCMVCGC-KCCRC SKCCKNL---EEEEKEQDVPVKA----SG
Lamprey SLC34a	TWNFLPDWMHSMKPLDRVISAVCG----- RCKKC ----- C ----- KCVSKSGK ----- NKQ VEVVISIPDST-----
Zebrafish Slc34a2b	SWDFLPLWAHSLDPDRVVTVIAA----- RCCCC ----- C ----- KCCNSNEEDEKAKLENLANGIE INDNT-----
Stickleback Slc34a2b	SWDFLPLWAHSLSPWDKVVGVFTA----- KCCCC ----- C ----- KCCQFADD -----DKETGETESLENNKSHT
Pufferfish Slc34a2a	SWDFLPRPLHSLAPWDVVTSM LG-FCGN RCCCC ----- C ----- KCSNCCQR -----NDEEAVR---KGS---LE
Stickleback Slc34a2a	SWDFLPRPMRSLAPWDVVTSAFG-FCGK HCCCC ----- C ----- KCKCKCRK -----KEDEKVMNQGRKS---LE
Zebrafish Slc34a2a	SWEFLPKPLHSLKPWDRVVTAGMS-FCRT RCCCC ----- C ----- KCCR -----NEEKNHMENNDRS---LE
Gar Slc34a2	TWEFLPKWMHSLKPWDVITSM LS-FCRT RCCCC ----- C ----- KCCNKIS -----SEEDGTGKEKGRS---LE
Coelacanth Slc34a2	TWDFLPLWMHSLHPWDKVITSM MG-YCGS HCKKC ----- C ----- KCCR-MVH -----AEDAGVKEKQVES---LH
Elephant Shark Slc34a2	TWKFLPIWLRSLPWRVDRVMQRFTD---IFCCCC-----K----- KC ----- SNKMK KEKGIKS---FE
Lizard Slc34a2	NWGFLPKWMRSLPWDNVVTSVSS-TCG RCCCC ----- C ----- KCCR ---RD-----KGEDVAKEKPTKS---LE
Chicken Slc34a2	NWDFLPIWMHSLPWDNMIMSSLA-FCGK HCCGF ----- C ----- KCKVN -----AEQEGAKDNQLKT---ME
Cow Slc34a3	SWAWLPLWLRSLPWDLLVRR-----CCPC-----KACSPQAVAKE-----TH
Opossum Slc34a3	SWAWLPLWLHSLQPWDRAITG-----CCPC-----CPRAHH-----EDSAGAALKE-----AQ
Elephant Slc34a3	SWAWLPHWLHSLPWDGLVTH-----CCPC-----QACSAPHATTKK-----AH
Human Slc34a3	SWAWLPLWLHSLPWDRLVTR-----CCPC-----NVCSPPKATTKE-----AY
Mouse Slc34a3	SWAWLPLWLHSLPWDRLVTA-----CCPC-----RACSNPMTSKV-----AH
Rat Slc34a3	SWAWLPLWLHSLPWDRLVTG-----CCPF-----KAYNSHMTSKV-----AH
Coelacanth Slc34a3	TWNFLPMWMHSLKPWDRLFSA-----CCT-----NCFKCKKQEGKGNSTAAAATELETAFGYNEPH
Frog Slc34a3	DWGFLPTWMHSLAPLDRLFSSVCG-----CCC-----KCCNKS-----EEEKPKQLPADLSLGMH